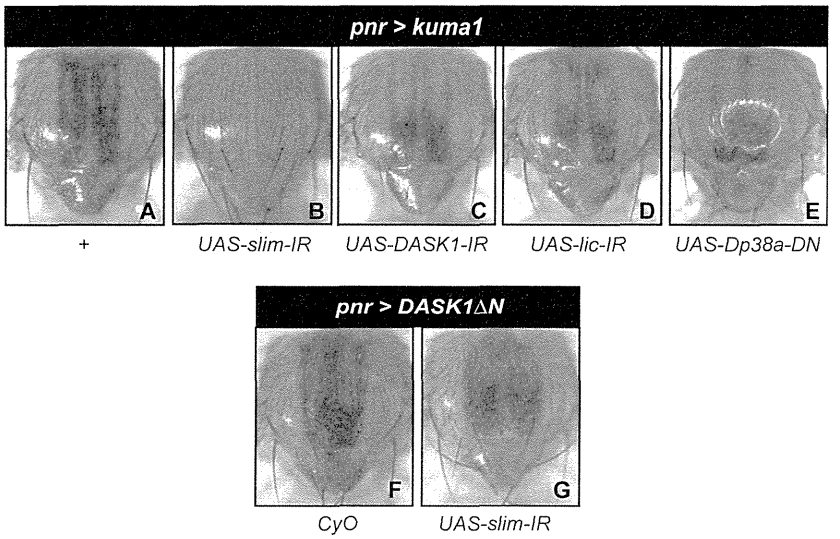

Figure 2. The DASK1-Dp38 Pathway Is Required for the Slim-Induced Melanization
Thoraxes of female flies with the following genotypes are shown: *kuma1/+*; *pnr-GAL4/+* (A), *kuma1/UAS-slim-IR*; *pnr-GAL4/+* (B), *kuma1/+*; *pnr-GAL4/UAS-DASK1-IR* (C), *kuma1/UAS-lic-IR*; *pnr-GAL4/+* (D), *UAS-Dp38a-DN/+*; *kuma1/+*; *pnr-GAL4/+* (E), *UAS-DASK1ΔN/CyO*; *pnr-GAL4/+* (F), and *UAS-DASK1ΔN/UAS-slim-IR*; *pnr-GAL4/+* (G).

KLHDC10 is mostly composed of the kelch repeat domain that consists of six repeated kelch motifs (Figure S1B). The amino acid sequence identity of the kelch repeat domain between Slim and KLHDC10 is 40.8%. Coexpression of Flag-tagged human KLHDC10 and human ASK1 in HEK293 cells also induced the activation of ASK1 and the subsequent activation of endogenous JNK and p38 (Figure 3B, compare lane 5 with lane 7). The fold increases in p-ASK1, p-p38, and p-JNK (upper band, p54) signals with KLHDC10 expression were shown in Figure 3C. These results suggest that Slim and KLHDC10 are evolutionarily conserved activators of the ASK1-MAPK cascades.

Slim/KLHDC10 Is a Substrate Recognition Subunit of the CRL2 Complex

Recent reports using mass spectrometry-based proteomic analyses revealed that several kelch domain-containing proteins including KLHDC2, KLHDC3, and KLHDC10 interacted with the Cullin2-RING ubiquitin ligase (CRL2) complex (Bennett et al., 2010; Mahrour et al., 2008). The CRL2 complex is composed of a large scaffold protein (Cullin2), a RING domain containing protein (Rbx1), adaptor proteins (Elongin B and Elongin C), a ubiquitin-like molecule (Nedd8), and a substrate recognition subunit (Bosu and Kipreos, 2008; Petroski and Deshaies, 2005). We confirmed the interaction of endogenous KLHDC10 with Cullin2 in Neuro2A cells (Figure S2A). Moreover, endogenous KLHDC10 was immunoprecipitated with Flag-Elongin B or Flag-Elongin C (Figure S2B), indicating that KLHDC10 is part of the CRL2 complex. KLHDC2 has been shown to possess the consensus sequence required for binding to Cullin2 or Elongin B and C, called the Cul2 box and the BC box, respectively, suggesting that KLHDC2 serves as one of the substrate recognition subunits of the CRL2 complex (Mahrour et al., 2008). We identified Cul2 box- and BC box-like sequences in the C-terminal region of Slim and KLHDC10 by comparison with those in KLHDC2 (Figure 4A) and constructed KLHDC10 mutants lacking the C-terminal region containing the Cul2 box and BC box sequences (ΔBC) or possessing a point mutation in the BC box (A409P; AP) (Figure 4B). We examined the ability of these mutants to bind to Cullin2. Endogenous Cullin2 was immunoprecipitated with Flag-tagged KLHDC10 WT, but not with Flag-KLHDC10 ΔBC or with AP mutants in HEK293 cells (Figure 4C). Cullin2 was detected as doublet bands; the upper and lower bands are known to correspond to the Nedd8-bound and unbound form of Cullin2, respectively (Jubelin et al., 2010). We also examined the interaction of Slim WT and the ΔBC mutant with the *Drosophila* CRL2 complex components, *Drosophila* Elongin C (dElongin C). Slim WT, but not the ΔBC mutant, interacted with dElongin C (Figure 4D). Moreover, we found that knockdown of *Cullin2* or *Drosophila Cullin2* (*dCul2*) resulted in the increase in protein levels of KLHDC10 or Slim, respectively (Figures S2C–S2E). The substrate recognition subunits of the CRL complex themselves have been known to be degraded through autoubiqutination by the CRL complex (Kamura et al., 2002), suggesting that Slim and KLHDC10 themselves are also regulated by the CRL2 complex. These results suggest that Slim and KLHDC10 function as one of the substrate recognition subunits of the CRL2 complex.

The CRL2 Complex Is Dispensable for Slim/KLHDC10-Dependent ASK1 Activation

To investigate whether Slim/KLHDC10-induced ASK1 activation requires the activity of Slim/KLHDC10 as the substrate recognition subunit in the CRL2 complex, we examined whether Slim/KLHDC10 mutants that failed to interact with the CRL2 complex could also activate DASK1. Interestingly, DASK1 was activated by the coexpression of Slim ΔBC as well as Slim WT (Figure 4E and Figure S2F). KLHDC10 AP mutant also activated ASK1 (Figure 4F), suggesting that Slim/KLHDC10 activates ASK1 in a CRL2 complex-independent manner. Because we have previously reported that ASK1 protein is degraded through ubiquitin-proteasome system upon H_2O_2 stimulation (Nagai et al., 2009), we also investigated the possibility that the CRL2-KLHDC10 complex regulates the stability of ASK1; however, knockdown of neither *KLHDC10* nor *Cullin2* affected the H_2O_2-dependent degradation of ASK1 (Figures S2G and S2H).

KLHDC10 Interacts with PP5 through Phosphatase Domain of PP5

To address the question of how Slim/KLHDC10 activates ASK1, we explored binding partners of KLHDC10 with a pull-down

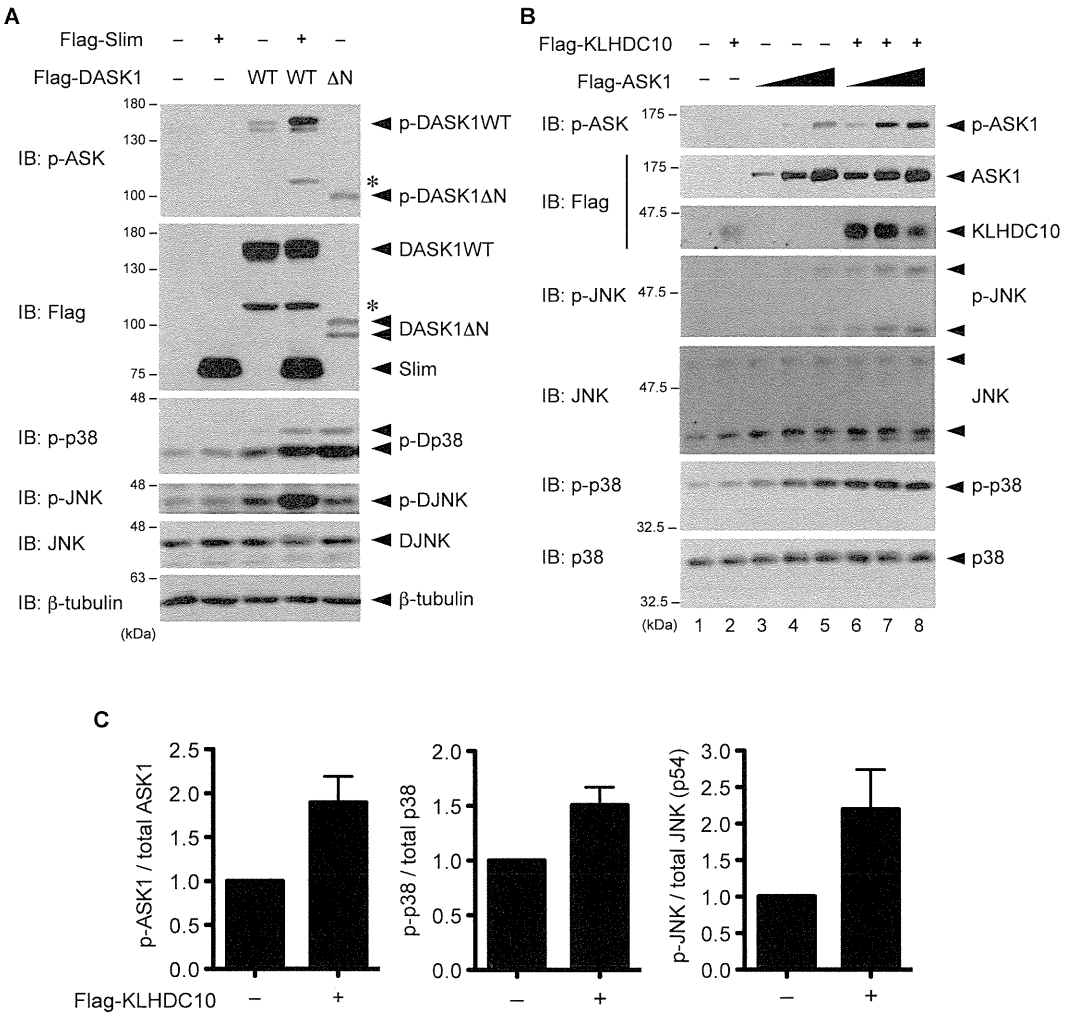

Figure 3. Slim/KLHDC10 Activates DASK1/ASK1

(A) S2 cells were transiently transfected with the indicated constructs and pWAGAL4. After 24 hr, cells were lysed and subjected to immunoblotting (IB). The asterisk indicates the putative C-terminal cleaved products of Flag-DASK1WT, which was observed when DASK1 WT was overexpressed in S2 cells. The lower band of Flag-DASK1 ΔN appeared to be a dephosphorylated form of DASK1 ΔN, because the upper but not lower band was detected by the phospho-ASK antibody.

(B) HEK293 cells were transiently transfected with the indicated constructs. After 24 hr, cells were lysed and subjected to IB.

(C) The ratios of phospho-ASK1, p38, and JNK (upper band; p54) to total ASK1, p38, and JNK (p54), respectively, with or without Flag-KLHDC10 expression were calculated and are shown as the fold changes. The results shown are the means of at least three independent experiments, and error bar indicates SEM.

screen using Flag-tagged KLHDC10 WT, ΔBC, or AP expressed in HEK293 cells as bait. As expected, multiple components of the CRL2 complex were pulled down with KLHDC10 WT, but not with the ΔBC and AP mutants (Table S1). We also identified several proteins that bound to the KLHDC10 ΔBC and AP mutants. Of these, we focused on a serine/threonine protein phosphatase, PP5, because we previously identified PP5 as a negative regulator of ASK1 (Morita et al., 2001). Coimmunoprecipitation analysis in HEK293 cells revealed that Flag-KLHDC10 WT, ΔBC, and A409P bound to coexpressed HA-PP5 (Figure 5A), suggesting that the interaction of KLHDC10 with the CRL2 complex is dispensable for the interaction of KLHDC10 with PP5. We also examined two other constructs; one is a deletion mutant of human KLHDC10 (KLHDC10 ΔN), which lacks the N-terminal 85 amino acids adjacent to the kelch repeat domain, and the other is a splicing variant of mouse KLHDC10 (KLHDC10 ΔE2), which skips exon 2 of the mouse *KLHDC10* gene and thus lacks the N-terminal 29 amino acids adjacent to the kelch repeat domain (Figure 4B). Both KLHDC10 ΔN and ΔE2 also bound to HA-PP5 (Figure 5A), suggesting that KLHDC10 interacted with PP5 through the six-repeated kelch motif. Because PP5 has been shown to localize to both nucleus and cytoplasm (Borthwick et al., 2001; Morita et al., 2001), we investigated the subcellular localization of Flag-KLHDC10 WT

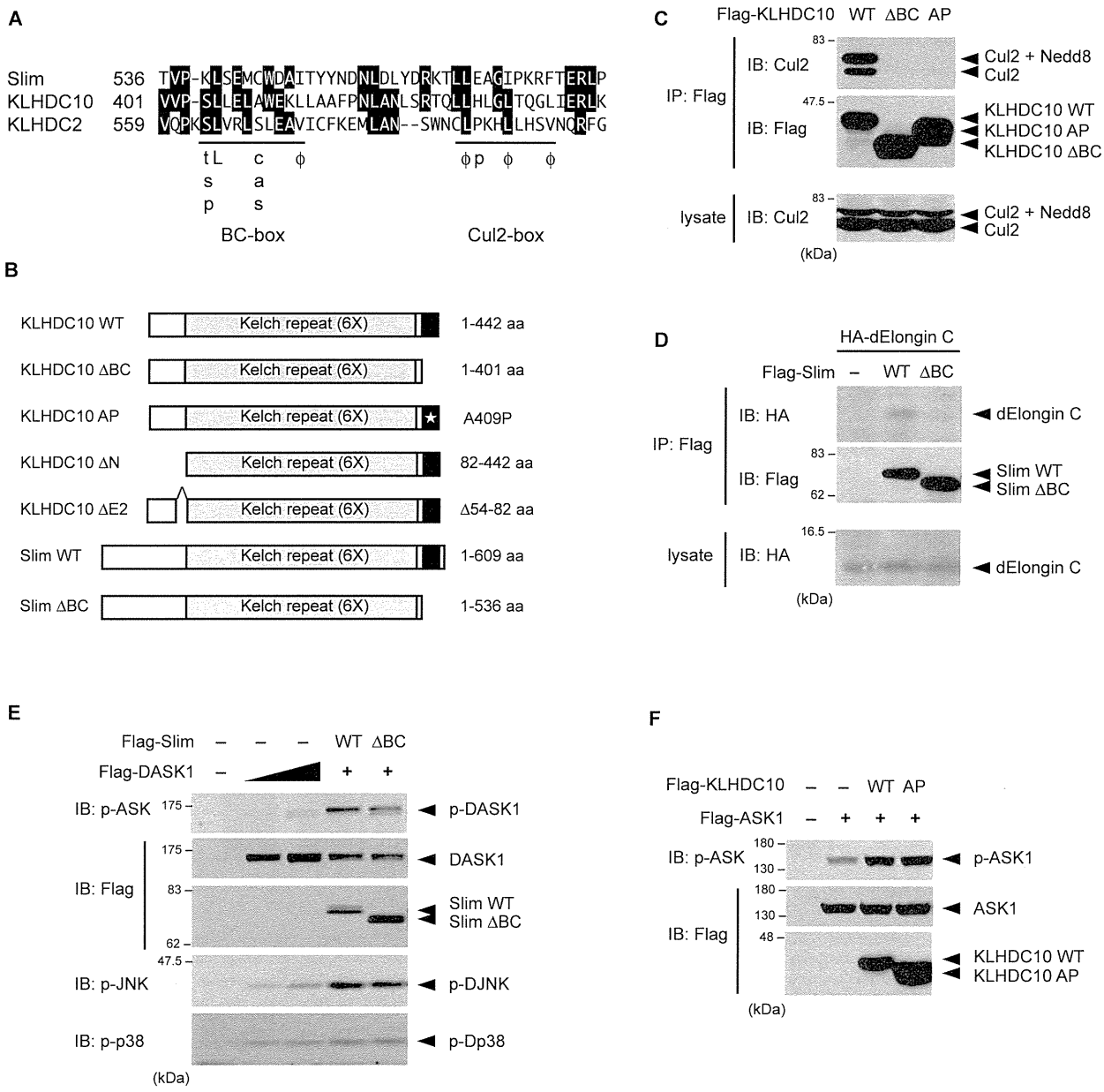

Figure 4. The CRL2 Complex Is Dispensable for ASK1 Activation by Slim

(A) ClustalW alignment of the amino acid sequences of the C-terminal regions of Slim, KLHDC10, and KLHDC2. Slim and KLHDC10 contain BC box- and Cul2 box-like sequences. ϕ indicates hydrophobic amino acids.

(B) Schematic representation of human KLHDC10 WT and its mutants ΔBC, AP, and ΔN and a splicing variant of mouse KLHDC10, ΔEx2, as well as Slim WT and ΔBC.

(C) HEK293 cells were transiently transfected with the indicated constructs. After 24 hr, cells were lysed and subjected to immunoprecipitation (IP) with anti-Flag antibody followed by immunoblotting (IB).

(D) Neuro2A cells were transiently transfected with the indicated constructs. After 24 hr, cells were lysed and subjected to IP with anti-Flag antibody followed by IB.

(E) S2 cells were transiently transfected with the indicated constructs and pWAGAL4. After 24 hr, the cells were lysed and subjected to IB.

(F) HEK293 cells were transiently transfected with the indicated constructs. After 24 hr, the cells were lysed and subjected to IB.

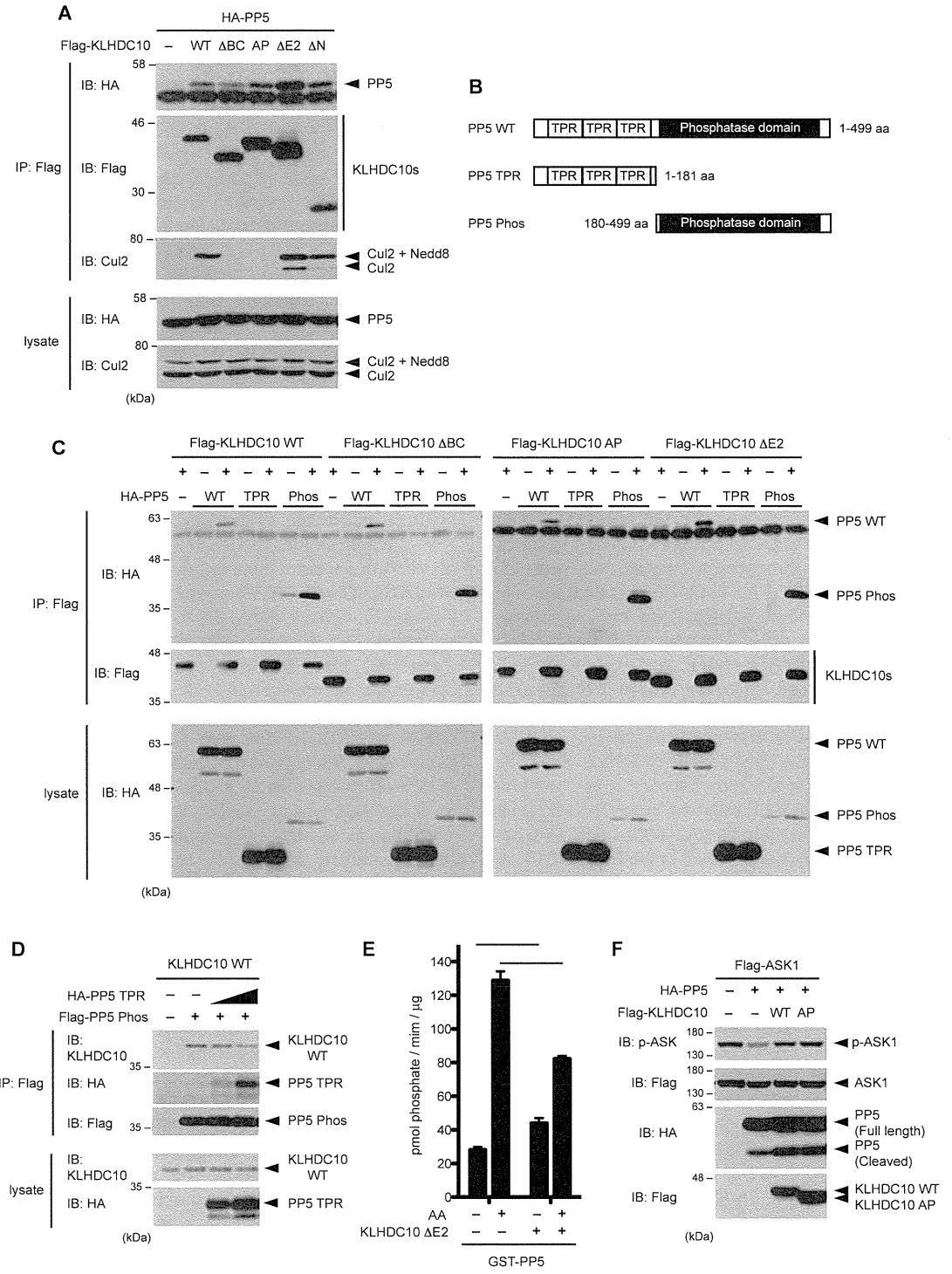

Figure 5. KLHDC10 Interacts with PP5 and Suppresses the Phosphatase Activity of PP5

(A) HEK293 cells were transiently transfected with the indicated constructs. After 48 hr, cells were lysed and subjected to immunoprecipitation (IP) with anti-Flag antibody followed by immunoblotting (IB).

(B) Schematic representation of human PP5 WT and its deletion mutants, TPR and Phos.

(C) HEK293 cells were transiently transfected with the indicated constructs. After 48 hr, cells were lysed and subjected to IP with anti-Flag antibody followed by IB.

and ΔE2. KLHDC10 WT localized predominantly to the nucleus but also to cytoplasm, whereas KLHDC10 ΔE2 exhibited cytoplasmic but not nuclear localization (Figures S3A and S3B), suggesting that nuclear localization of KLHDC10 is regulated via the amino acid sequence within the exon2 region. A bipartite basic amino acids cluster, KKKIRWDPVRRR, included in this region may function as a nuclear localization signal for KLHDC10 (Figure S3C). These data indicate that KLHDC10 interacts with PP5 in both nucleus and cytoplasm.

KLHDC10 Regulates Phosphatase Activity of PP5

PP5 contains three consecutive TPR domains within its N-terminal region that are known to function as the autoinhibitory domain covering the catalytic site within the C-terminal phosphatase domain of PP5 (Yang et al., 2005). Based on a coimmunoprecipitation analysis using PP5 deletion constructs (Figure 5B), we found that all KLHDC10 constructs we tested preferentially bound to the C-terminal fragment of PP5 including the phosphatase domain (PP5 Phos), but not to the N-terminal fragment containing the TPR domain (PP5 TPR) (Figure 5C). In addition, the interaction between KLHDC10 and PP5 Phos was suppressed by further coexpression of PP5 TPR, indicating the possibility that KLHDC10 and PP5 TPR competitively interact with PP5 Phos through the catalytic site within the phosphatase domain of PP5 (Figure 5D). These results prompted us to examine the effect of KLHDC10 on the phosphatase activity of PP5. Glutathione S-transferase (GST)-fused recombinant PP5 protein was purified from *E. coli*, and phosphatase activity was measured by an in vitro phosphatase assay using the phosphothreonine peptide as a substrate. It has been shown that PP5 is activated by arachidonic acid (AA) through interaction with the TPR domain of PP5 in vitro (Chen and Cohen, 1997; Kang et al., 2001; Skinner et al., 1997). We confirmed that incubation of PP5 with AA increased PP5 phosphatase activity and found that this AA-induced GST-PP5 activation was suppressed in the presence of GST-KLHDC10 ΔE2 protein (Figure 5E). These results suggest that KLHDC10 possesses the ability to suppress the phosphatase activity of PP5 by interacting with the PP5 phosphatase domain. In contrast, the basal activity of PP5 was slightly but significantly increased with KLHDC10 ΔE2 (Figure 5E), which might be attributed to the basal binding of KLHDC10 to the phosphatase domain of PP5, interrupting the TPR domain-dependent autoinhibition of PP5.

PP5 dephosphorylates the phosphothreonine (Thr838) in the activation loop of human ASK1 kinase domain, inactivating ASK1 in response to ROS (Morita et al., 2001). Thus, we examined whether KLHDC10 counteracts PP5-dependent inactivation of ASK1. Coexpression of ASK1 and PP5 decreased the phosphorylation of ASK1 Thr838, indicating that ASK1 is inactivated by PP5 (Figure 5F). Under these conditions, coexpression of KLHDC10 WT or AP inhibited the PP5-induced dephosphorylation of ASK1 (Figure 5F). KLHDC10 also counteracted the PP5-dependent inactivation of ASK1 in H_2O_2-treated cells (Figure S3D). Furthermore, knockdown of *PP5* in HEK293 cells reduced the KLHDC10-induced activation of ASK1 (Figure S3E), suggesting that PP5-dependent inactivation of ASK1 is required at least in part for the KLHDC10-induced ASK1 activation. These results indicate that KLHDC10 activates ASK1 by inhibiting PP5-dependent inactivation of ASK1.

H_2O_2-Dependent Interaction of KLHDC10 with PP5

Because ASK1 interacts with PP5 in an H_2O_2-dependent manner, we examined whether the interaction of KLHDC10 with PP5 was also affected by H_2O_2 stimulation. The interaction of coexpressed KLHDC10 WT or AP with PP5 WT increased in response to H_2O_2 (Figure 6A). TNF-α, which has been reported to induce the activation of ASK1 through ROS production and the interaction of ASK1 with PP5 (Liu et al., 2000; Morita et al., 2001), also induced the increase in binding between KLHDC10 and PP5 (Figure S4A). This binding was attenuated with pretreatment of antioxidant, N-acetylcysteine (NAC), suggesting that TNF-α increased the interaction between KLHDC10 and PP5 in an ROS-dependent manner. In contrast, the interaction of KLHDC10 WT with PP5 Phos was not altered by H_2O_2 treatment (Figure 6B). Given that KLHDC10 strongly bound to PP5 Phos rather than PP5 WT even under conditions of no oxidative stress (Figure 5C), these results imply that ROS might induce some conformational changes in PP5 that unlock the autoinhibitory structure of PP5, thereby leading to an increase in the interaction between KLHDC10 and PP5 WT. In these immunoblotting experiments, we noticed that, upon H_2O_2 stimulation, a fraction of PP5 WT bands migrating faster than the major bands of PP5 on SDS-PAGE was increased (Figures 6A and 6B, lysate). The lower bands of both exogenous and endogenous PP5 were not detected by an antibody against the C terminus of PP5 (Figures S4B and S4C), indicating that H_2O_2 induces the C-terminal cleavage of a fraction of PP5. The putative cleavage site in the C terminus of PP5 has been reported to be located between Arg425 and Ser426 (Zeke et al., 2005). Although the C-terminal cleaved form derived from HA-PP5 WT was hardly detected in coIP with KLHDC10, probably due to relatively low amount of cleaved form compared with that of full-length form (Figure 6A), we found that KLHDC10 WT bound to the coexpressed putative cleaved form mutant (PP5 Δ426-499) (Figure S4D), suggesting that KLHDC10 interacts with both full-length and the cleaved form of PP5. In addition, we detected the interaction between endogenous KLHDC10 and PP5 in Neuro2A cells (Figure 6C). The total amount of PP5 (full length and cleaved) coimmunoprecipitated with KLHDC10

(D) HEK293 cells were transiently transfected with the indicated constructs. After 24 hr, cells were treated with 0.5 μM MG132 to enhance transfected protein expression. After an additional 14 hr of culturing, cells were lysed and subjected to IP with anti-Flag antibody followed by IB.
(E) GST-tagged recombinant PP5 and KLHDC10 ΔE2 were purified from *E. coli*. GST-PP5 alone or in combination with GST-KLHDC ΔE2, incubated with or without 400 μM AA at 30°C for 20 min, was subjected to an in vitro phosphatase assay using a phosphothreonine peptide as a substrate. The results shown are the means of three independent experiments. Error bars indicate SEM (*$p < 0.02$, **$p < 0.01$, Student's t test).
(F) HEK293 cells were transiently transfected with the indicated constructs. After 24 hr, the cells were lysed and subjected to IB. The asterisks in (A) and (C) indicate the bands derived from immunoglobulin heavy chain.

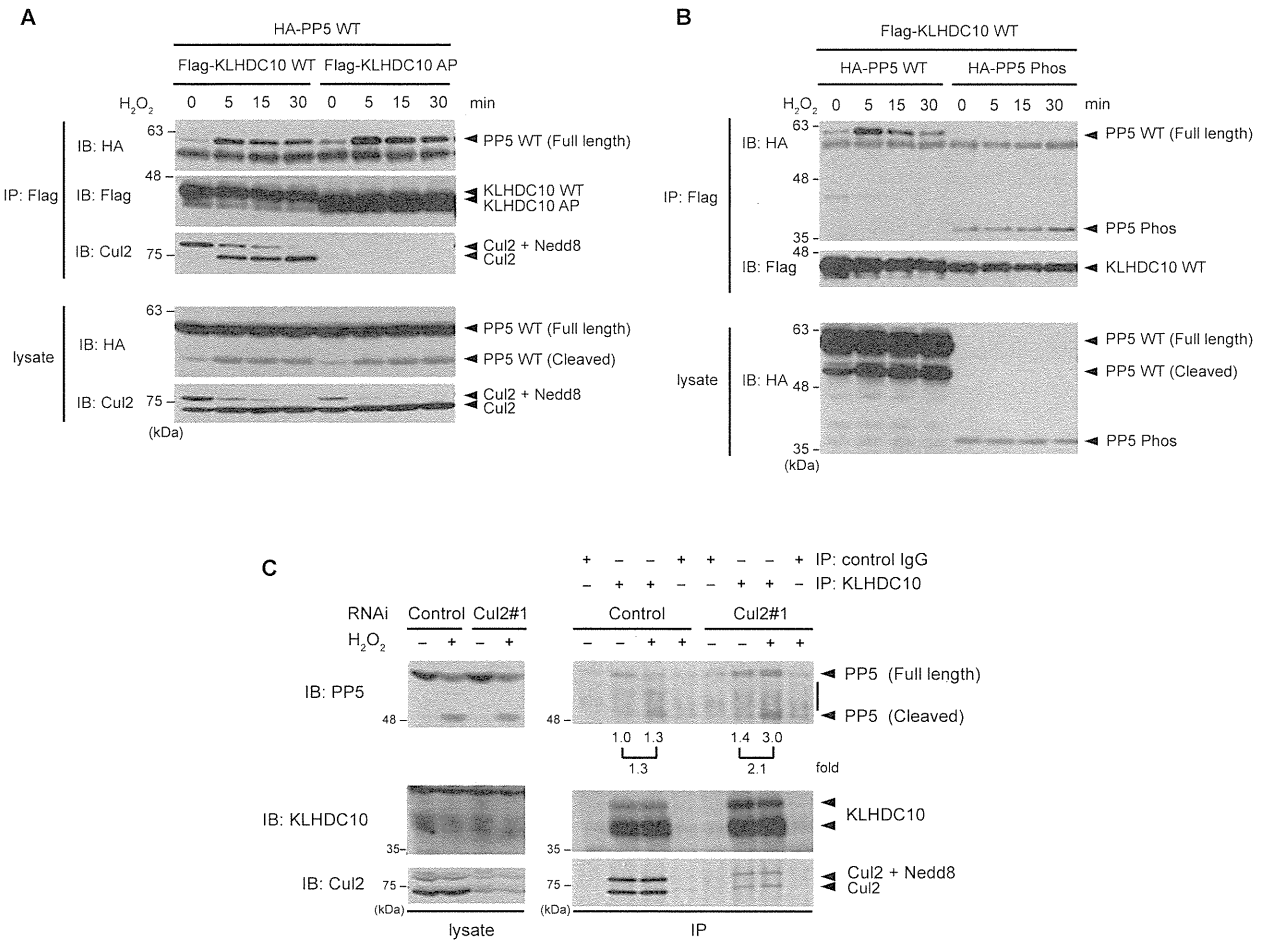

Figure 6. H_2O_2-Dependent Interaction of KLHDC10 with PP5

(A and B) HEK293 cells were transiently transfected with the indicated constructs. After 48 hr, the cells were treated with 5 mM H_2O_2 for the indicated periods and then lysed and subjected to immunoprecipitation (IP) with anti-Flag antibody followed by immunoblotting (IB).

(C) Neuro2A cells were transfected with a negative control siRNA or an siRNA that targets *Cul2*. After 48 hr, the cells were treated with 1 mM H_2O_2 for 1 hr and then lysed and subjected to IP with control IgG or KLHDC10 antibody followed by IB. The asterisk indicates the bands derived from immunoglobulin heavy chain or nonspecific bands. The total amount of PP5 (full length and cleaved) coimunoprecipitated with KLHDC10 was quantified and was shown as the fold changes.

was increased in response to H_2O_2. The interaction was also enhanced by knockdown of *Cullin2*, presumably reflecting the result that PP5 was isolated only from the pull-down of Cul2-unbound mutants of KLHDC10 (Figure 6C and Table S1).

KLHDC10 Is Required for H_2O_2-Induced Sustained Activation of ASK1 and Cell Death

Because the interaction of KLHDC10 with PP5 was induced by H_2O_2, we next examined the requirement for KLHDC10 in H_2O_2-induced ASK1 activation. Knockdown of *KLHDC10* in Neuro2A cells resulted in a decrease in H_2O_2-induced activation of ASK1, which was more remarkable in the late time course (60–120 min) than in the early time course (5–15 min) after H_2O_2 stimulation (Figure 7A and Figure S5A). H_2O_2-induced p38 activation was also decreased in *KLHDC10* knockdown cells. These results suggest that KLHDC10 is required for ROS-induced sustained activation but not for early (initial) activation of ASK1. Because the ASK1-p38 pathway is known to be crucial for ROS-induced cell death (Noguchi et al., 2008), we investigated the effect of knockdown of *KLHDC10* on H_2O_2-induced cell death in Neuro2A cells. LDH assay revealed that H_2O_2-induced cell death was significantly suppressed by knockdown of *KLHDC10* (Figure 7B), suggesting that KLHDC10 is required for ROS-induced cell death. Furthermore, to address the requirement of PP5 for KLHDC10-induced ASK1 activation and cell death, we examined the effect of *PP5* knockdown on H_2O_2-induced ASK1 activation in *KLHDC10* knockdown cells, in which ASK1 activation was supposed to be inhibited by "active" PP5. Knockdown of *PP5* restored the activation of ASK1 in H_2O_2-treated *KLHDC10* knockdown cells to the level of that in control knockdown cells (Figure 7C, Figures S5B and S5C), suggesting that suppression of ASK1 activation in *KLHDC10* knockdown cells is mostly dependent on PP5. H_2O_2-induced cell death was also restored by *KLHDC10* and

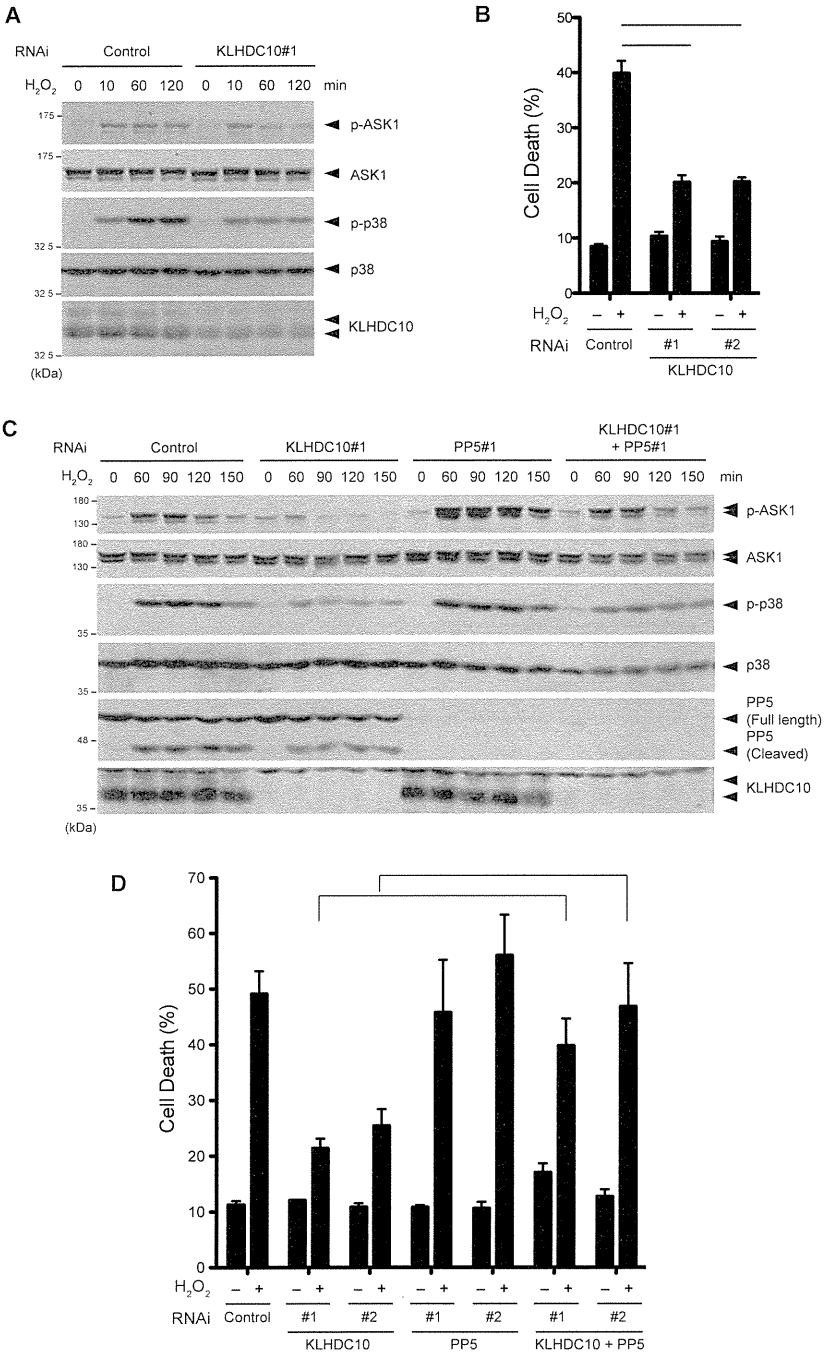

Figure 7. KLHDC10 Is Required for H_2O_2-Induced Activation of ASK1 and Cell Death

(A and B) Neuro2A cells were transfected with a negative control siRNA or an siRNA that targets *KLHDC10*. After 48 hr, the cells were treated with 0.5 mM H_2O_2 for the indicated periods, then lysed and subjected to immunoblotting (IB) with the indicated antibodies (A), or after 43 hr, the cells were treated with 1 mM H_2O_2 for 5 hr and then analyzed with an LDH assay (B). The results shown are the means of three independent experiments. Error bars indicate SEM (**$p < 0.003$, ***$p < 0.007$, Student's t test).

(C and D) Neuro2A cells were transfected with the indicated siRNAs. After 48 hr, the cells were harvested and replated. After 24 hr, the indicated siRNAs were transfected again. After 48 hr, the cells were treated with 0.5 mM H_2O_2 for the indicated periods and then lysed and subjected to IB (C), or after 43 hr, the cells were treated with 1 mM H_2O_2 for 5 hr and then analyzed with an LDH assay (D). The results shown are the means of at least five independent experiments. Error bars indicate SEM (*$p < 0.05$, Student's t test). The asterisk indicates nonspecific bands.

PP5 double knockdown (Figure 7D). These results strongly suggest that suppression of PP5 is crucial for the KLHDC10-induced ASK1 activation and cell death.

DISCUSSION

Recent reports have shed light on the role of the kelch repeat proteins as the substrate recognition subunits of the CRL complex (Bennett et al., 2010). We also confirmed the interaction of Slim/KLHDC10 with the components of the CRL2 complex through the BC box and Cul2 box sequences (Figures 4C and 4D), suggesting that Slim/KLHDC10 functions as one of the substrate recognition subunits of the CRL2 complex. However, interestingly, the function of Slim/KLHDC10 as the ASK1 activator appeared to be independent of the interactions of the CRL2 complex (Figures 4E and 4F). This finding suggests that Slim/KLHDC10 possesses at least two functions, one as a substrate recognition subunit that targets unidentified substrates for ubiquitination, and another as a signaling regulator through its interaction with PP5. A tumor suppressor gene product, the von Hippel-Lindau protein (pVHL), is one of the most characterized substrate recognition subunits of the CRL2 complex. It has been shown that pVHL binds to a transcription factor, hypoxia-inducible factor-1α (HIF-1α), in an oxygen concentration-dependent manner, allowing the CRL2-pVHL complex to mediate ubiquitination and degradation of HIF-1α (Kaelin, 2008). Moreover, pVHL is also reported to play a CRL2 complex-independent role via its interaction with various molecules, such as fibronectin, Collagen IV, and kinesin-2 (Frew and Krek, 2008). These findings suggest that pVHL is a multifunctional protein and that its function depends on its binding partners. Our findings also suggest that KLHDC10 might

possess multiple functions through the interaction with other binding molecules identified by the pull-down screen in this study (Table S1).

We demonstrated that KLHDC10 is an inhibitor of PP5. Given the importance of the balance between kinases and phosphatases in various intracellular signaling systems, it is indisputable that not only kinases but also phosphatases need to be tightly regulated by their regulatory molecules. It has been shown that PP5 is activated by heat shock protein 90 (HSP90) through an interaction of the C-terminal region of HSP90 and the TPR domain of PP5, and this interaction disrupts the autoinhibitory structure of PP5 (Yang et al., 2005). The HSP90-PP5 complex targets HSP90-associated proteins, such as the glucocorticoid receptor and heme-regulated eIF2α kinase, for dephosphorylation, thereby regulating their molecular functions (Golden et al., 2008). The G_{12} class of G protein members, $G\alpha_{12}$ and $G\alpha_{13}$, has also been shown to activate PP5 catalytic activity by associating with the TPR domain of PP5 (Yamaguchi et al., 2002). In contrast, although PP5 exhibits weak phosphatase activity, owing to its autoinhibitory structure, little is known about the negative regulatory mechanism of PP5 by inhibitory proteins. We revealed that KLHDC10 interacted with the PP5 Phos and that this interaction was suppressed by the TPR domain of PP5 (Figures 5C and 5D). Because the TPR domain of PP5 has been shown to directly associate with the catalytic site of the phosphatase domain (Yang et al., 2005), these findings suggest that KLHDC10 inhibits PP5 phosphatase activity by interacting with the catalytic site of PP5. Consistent with this notion, KLHDC10 suppressed the AA-activated phosphatase activity but not the basal activity of PP5 (Figure 5E). Because AA has been shown to induce the activation of PP5 by disrupting the autoinhibitory structure of PP5 through direct interaction with the TPR domain, this suggests that AA-induced conformational change of PP5 that opens up the catalytic site of PP5 triggers the KLHDC10-PP5 interaction to inhibit the catalytic activity of PP5.

H_2O_2 increased the interaction of KLHDC10 with PP5 WT, whereas KLHDC10 constitutively bound to PP5 Phos regardless of the presence of H_2O_2 (Figures 6A and 6B). In addition, H_2O_2 induced the C-terminal cleavage of a fraction of PP5 (Figure 6 and Figure S4C). The three-dimensional structure of PP5 has revealed that together with the TPR domain, the α helix structure at the C-terminal of PP5 is also involved in its autoinhibitory structure (Yang et al., 2005). Thus, the cleavage of the C terminus of PP5 indicates that the catalytic site of the phosphatase domain of PP5 is uncovered upon H_2O_2, which is consistent with the finding that KLHDC10 preferentially interacted with the cleaved form of PP5 (Figure 6C and Figure S4D). Although coexpression of KLHDC10 did not affect the cleavage of PP5 (Figure S4B), it would be interesting in the future to examine the effect of C-terminal cleavage on the phosphatase activity of PP5 by using deletion constructs. However, because KLHDC10 bound even to the full-length form of PP5 in an H_2O_2-dependent manner, the cleavage of PP5 itself seems to be dispensable for the H_2O_2-dependent interaction of KLHDC10 with PP5 (Figure 5 and Figure 6). Nevertheless, in response to H_2O_2, certain conformational change in PP5 that precedes the C-terminal cleavage might induce the open-up of PP5 phosphatase domain and eventually the interaction of KLHDC10 with PP5.

Knockdown of *KLHDC10* in Neuro2A cells resulted in a decrease in H_2O_2-dependent sustained activation of ASK1 and cell death (Figure 7). We have recently identified the deubiquitinating enzyme ubiquitin-specific peptidase 9, X-linked (USP9X) as an H_2O_2-dependent binding molecule of ASK1 (Nagai et al., 2009). USP9X interacts with ASK1 via its ubiquitin-like sequence (LRLRGG), which is identical to the ubiquitin C terminus. USP9X binds within the C-terminal region of ASK1 and removes the ubiquitin from the activated ASK1, thereby leading to stabilization of the activated ASK1. USP9X is also required for oxidative stress-induced cell death. These findings and the findings in this study raise the possibility that USP9X and KLHDC10 may coordinately regulate the strength and/or duration of ASK1 activation by counteracting both ubiquitination of ASK1 by ubiquitin ligases and dephosphorylation of ASK1 by PP5, leading to sustained activation of ASK1 and ultimately cell death. Because ROS-activated ASK1 has been known to mediate not only cell death but also various cellular responses including inflammatory responses and cardiac hypertrophy in a stimulus- and cellular context-dependent manner (Iriyama et al., 2009; Izumiya et al., 2003; Matsuzawa et al., 2005; Noguchi et al., 2008), such fine-tuning of the magnitude of ASK1 activation by USP9X and KLHDC10 seems to be a crucial determinant of ASK1-mediated cellular responses to oxidative stress. Further analyses of physiological and/or pathological contexts in which ROS-dependent KLHDC10-PP5 interaction regulates the activation of ASK1 will provide new insight into ROS- and ASK1-mediated stress responses and human diseases.

EXPERIMENTAL PROCEDURES

Additional information regarding plasmids, antibodies, cell culture, RNA interference, quantitative RT-PCR, immunostaining, and mass spectrometry analysis can be found in the Supplemental Experimental Procedures.

Fly Stocks and Generation of Transgenic Flies

Flies were raised on standard *Drosophila* medium at 25°C. The GS strains were provided by the *Drosophila* Genetic Research Center at Kyoto Institute of Technology. The following strains were used in this study: *UAS-DASK1ΔN*, *UAS-DASK1-IR* (Sekine et al., 2011), *UAS-Dp38a-DN* (Adachi-Yamada et al., 1999), *UAS-lic-IR* (Vienna *Drosophila* RNAi Center), *pnr-GAL4* (Calleja et al., 2000), *UAS-GFP^{S65T}*, and *hs-GAL4* (Bloomington *Drosophila* Stock Center). The transgenic strains harboring *UAS-DASK1WT* (Kuranaga et al., 2002) and *UAS-slim-IR* were generated through standard P element-mediated transformation (BestGene Inc.).

Immunoblotting Analysis

Cells were lysed in IP lysis buffer (50 mM Tris-HCl [pH 7.5], 150 mM NaCl, 1% Triton X-100, 1% deoxycholate, 10 mM EDTA, and 1 mM phenylmethylsulfonyl fluoride [PMSF] in addition to 150 units/ml of aprotinin or 5 mg/ml leupeptin) supplemented with PhosSTOP (Roche). Flies were lysed with RIPA buffer (1% Nonidet P-40, 0.5% deoxycholate, 0.1% SDS, 50 mM Tris-HCl [pH 8.0], 150 mM NaCl, 1 mM PMSF, and 5 μg/ml leupeptin). The cell and fly extracts were clarified by centrifugation, and the supernatants were added to the same volume of SDS sample buffer (40 mM Tris-HCl [pH 8.8], 80 μg/ml bromophenol blue, 28.8% glycerol, 4% SDS, and 20 mM DTT with or without 5% 2-mercaptoethanol), boiled at 98°C for 5 min, resolved on SDS-polyacrylamide gel electrophoresis (SDS-PAGE), and electroblotted onto polyvinylidene difluoride (PVDF) membranes. After blocking with 5% skim milk in TBS-T (50 mM Tris-HCl [pH 8.0], 150 mM NaCl, and 0.05% Tween 20), the

membranes were probed with the indicated antibodies. The antibody-antigen complexes were detected using the ECL system (GE Healthcare). The optical density of bands was quantified using NIH ImageJ software. All immunoblotting data are representative of at least three independent experiments.

Coimmunoprecipitation Analysis

Cells were lysed in IP lysis buffer. After centrifugation, the supernatants were immunoprecipitated with Flag antibody (anti-Flag affinity M2 gel, Sigma). The beads were extensively washed with IP lysis buffer before immunoblotting analysis. For IP of endogenous KLHDC10, Neuro2A cell lysates were incubated with control rat IgG (Santa Cruz) or KLHDC10 antibody (clone S-20, Supplemental Experimental Procedures) and immunoprecipitated with protein G Sepharose (GE Healthcare).

In Vitro Phosphatase Assay

The GST-PP5 and GST-KLHDC10 ΔE2 proteins were purified from *E. coli* (BL21) as described previously (Saitoh et al., 1998). GST-PP5 (0.4 μg) alone or in combination with GST-KLHDC10 ΔE2 (5 μg) in 50 μl reaction mixture (approximately 0.1 and 1.4 μM, respectively) was incubated with 25 μM phospho-threonine peptide (RRApTVA, Promega) at 30°C for 20 min with or without 400 μM AA. The phosphatase activity of PP5 was measured using the Serine/Threonine Phosphatase Assay System (Promega), which determined the absorbance of a molybdate:malachite:phosphate complex.

LDH Assay

H_2O_2-induced cell death was monitored using the LDH-Cytotoxic Test Wako (Wako) according to the manufacturer's protocols. The released LDH activity into the culture media was quantified as a percentage of the total LDH activity.

Statistical Analysis

Statistical analyses were performed using Student's t test.

SUPPLEMENTAL INFORMATION

Supplemental Information includes five figures, one table, Supplemental Experimental Procedures, and Supplemental References and can be found with this article at http://dx.doi.org/10.1016/j.molcel.2012.09.018.

ACKNOWLEDGMENTS

We thank T. Adachi-Yamada, T. Aigaki, and S.B. Carroll for fly strains; Y. Hiromi and R. Ueda for plasmids; and the Bloomington *Drosophila* Stock Center, the *Drosophila* Genetic Resource Center at Kyoto Institute of Technology, NIG-FLY stock center, and the Vienna *Drosophila* RNAi Center for fly strains. We are grateful to all the members of the Laboratory of Cell Signaling for their critical comments. This work was supported by KAKENHI from JSPS and MEXT, Strategic Approach to Drug Discovery and Development in Pharmaceutical Sciences, GCOE Program, the "Understanding of molecular and environmental bases for brain health" conducted under the Strategic Research Program for Brain Sciences by MEXT, the Advanced Research for Medical Products Mining Programme of the National Institute of Biomedical Innovation, the Naito Foundation Natural Science Scholarship, the Cosmetology Research Foundation, and the Tokyo Biochemical Research Foundation.

Received: October 10, 2011
Revised: July 25, 2012
Accepted: September 11, 2012
Published online: October 25, 2012

REFERENCES

Adachi-Yamada, T., Nakamura, M., Irie, K., Tomoyasu, Y., Sano, Y., Mori, E., Goto, S., Ueno, N., Nishida, Y., and Matsumoto, K. (1999). p38 mitogen-activated protein kinase can be involved in transforming growth factor beta superfamily signal transduction in Drosophila wing morphogenesis. Mol. Cell. Biol. *19*, 2322–2329.

Adams, J., Kelso, R., and Cooley, L. (2000). The kelch repeat superfamily of proteins: propellers of cell function. Trends Cell Biol. *10*, 17–24.

Bennett, E.J., Rush, J., Gygi, S.P., and Harper, J.W. (2010). Dynamics of cullin-RING ubiquitin ligase network revealed by systematic quantitative proteomics. Cell *143*, 951–965.

Borthwick, E.B., Zeke, T., Prescott, A.R., and Cohen, P.T. (2001). Nuclear localization of protein phosphatase 5 is dependent on the carboxy-terminal region. FEBS Lett. *491*, 279–284.

Bosu, D.R., and Kipreos, E.T. (2008). Cullin-RING ubiquitin ligases: global regulation and activation cycles. Cell Div. *3*, 7.

Brand, A.H., and Perrimon, N. (1993). Targeted gene expression as a means of altering cell fates and generating dominant phenotypes. Development *118*, 401–415.

Calleja, M., Herranz, H., Estella, C., Casal, J., Lawrence, P., Simpson, P., and Morata, G. (2000). Generation of medial and lateral dorsal body domains by the pannier gene of Drosophila. Development *127*, 3971–3980.

Chen, M.X., and Cohen, P.T. (1997). Activation of protein phosphatase 5 by limited proteolysis or the binding of polyunsaturated fatty acids to the TPR domain. FEBS Lett. *400*, 136–140.

Finkel, T., and Holbrook, N.J. (2000). Oxidants, oxidative stress and the biology of ageing. Nature *408*, 239–247.

Frew, I.J., and Krek, W. (2008). pVHL: a multipurpose adaptor protein. Sci. Signal. *1*, pe30. http://dx.doi.org/10.1126/scisignal.124pe30.

Fujino, G., Noguchi, T., Matsuzawa, A., Yamauchi, S., Saitoh, M., Takeda, K., and Ichijo, H. (2007). Thioredoxin and TRAF family proteins regulate reactive oxygen species-dependent activation of ASK1 through reciprocal modulation of the N-terminal homophilic interaction of ASK1. Mol. Cell. Biol. *27*, 8152–8163.

Golden, T., Swingle, M., and Honkanen, R.E. (2008). The role of serine/threonine protein phosphatase type 5 (PP5) in the regulation of stress-induced signaling networks and cancer. Cancer Metastasis Rev. *27*, 169–178.

Hinds, T.D., Jr., and Sánchez, E.R. (2008). Protein phosphatase 5. Int. J. Biochem. Cell Biol. *40*, 2358–2362.

Ichijo, H., Nishida, E., Irie, K., ten Dijke, P., Saitoh, M., Moriguchi, T., Takagi, M., Matsumoto, K., Miyazono, K., and Gotoh, Y. (1997). Induction of apoptosis by ASK1, a mammalian MAPKKK that activates SAPK/JNK and p38 signaling pathways. Science *275*, 90–94.

Iriyama, T., Takeda, K., Nakamura, H., Morimoto, Y., Kuroiwa, T., Mizukami, J., Umeda, T., Noguchi, T., Naguro, I., Nishitoh, H., et al. (2009). ASK1 and ASK2 differentially regulate the counteracting roles of apoptosis and inflammation in tumorigenesis. EMBO J. *28*, 843–853.

Izumiya, Y., Kim, S., Izumi, Y., Yoshida, K., Yoshiyama, M., Matsuzawa, A., Ichijo, H., and Iwao, H. (2003). Apoptosis signal-regulating kinase 1 plays a pivotal role in angiotensin II-induced cardiac hypertrophy and remodeling. Circ. Res. *93*, 874–883.

Jubelin, G., Taieb, F., Duda, D.M., Hsu, Y., Samba-Louaka, A., Nobe, R., Penary, M., Watrin, C., Nougayrède, J.P., Schulman, B.A., et al. (2010). Pathogenic bacteria target NEDD8-conjugated cullins to hijack host-cell signaling pathways. PLoS Pathog. *6*, e1001128. http://dx.doi.org/10.1371/journal.ppat.1001128.

Kaelin, W.G., Jr. (2008). The von Hippel-Lindau tumour suppressor protein: O2 sensing and cancer. Nat. Rev. Cancer *8*, 865–873.

Kamura, T., Brower, C.S., Conaway, R.C., and Conaway, J.W. (2002). A molecular basis for stabilization of the von Hippel-Lindau (VHL) tumor suppressor protein by components of the VHL ubiquitin ligase. J. Biol. Chem. *277*, 30388–30393.

Kang, H., Sayner, S.L., Gross, K.L., Russell, L.C., and Chinkers, M. (2001). Identification of amino acids in the tetratricopeptide repeat and C-terminal domains of protein phosphatase 5 involved in autoinhibition and lipid activation. Biochemistry *40*, 10485–10490.

Kuranaga, E., Kanuka, H., Igaki, T., Sawamoto, K., Ichijo, H., Okano, H., and Miura, M. (2002). Reaper-mediated inhibition of DIAP1-induced DTRAF1

degradation results in activation of JNK in Drosophila. Nat. Cell Biol. *4*, 705–710.

Kyriakis, J.M., and Avruch, J. (2001). Mammalian mitogen-activated protein kinase signal transduction pathways activated by stress and inflammation. Physiol. Rev. *81*, 807–869.

Liu, H., Nishitoh, H., Ichijo, H., and Kyriakis, J.M. (2000). Activation of apoptosis signal-regulating kinase 1 (ASK1) by tumor necrosis factor receptor-associated factor 2 requires prior dissociation of the ASK1 inhibitor thioredoxin. Mol. Cell. Biol. *20*, 2198–2208.

Mahrour, N., Redwine, W.B., Florens, L., Swanson, S.K., Martin-Brown, S., Bradford, W.D., Staehling-Hampton, K., Washburn, M.P., Conaway, R.C., and Conaway, J.W. (2008). Characterization of Cullin-box sequences that direct recruitment of Cul2-Rbx1 and Cul5-Rbx2 modules to Elongin BC-based ubiquitin ligases. J. Biol. Chem. *283*, 8005–8013.

Matsuzawa, A., Saegusa, K., Noguchi, T., Sadamitsu, C., Nishitoh, H., Nagai, S., Koyasu, S., Matsumoto, K., Takeda, K., and Ichijo, H. (2005). ROS-dependent activation of the TRAF6-ASK1-p38 pathway is selectively required for TLR4-mediated innate immunity. Nat. Immunol. *6*, 587–592.

Morita, K., Saitoh, M., Tobiume, K., Matsuura, H., Enomoto, S., Nishitoh, H., and Ichijo, H. (2001). Negative feedback regulation of ASK1 by protein phosphatase 5 (PP5) in response to oxidative stress. EMBO J. *20*, 6028–6036.

Nagai, H., Noguchi, T., Takeda, K., and Ichijo, H. (2007). Pathophysiological roles of ASK1-MAP kinase signaling pathways. J. Biochem. Mol. Biol. *40*, 1–6.

Nagai, H., Noguchi, T., Homma, K., Katagiri, K., Takeda, K., Matsuzawa, A., and Ichijo, H. (2009). Ubiquitin-like sequence in ASK1 plays critical roles in the recognition and stabilization by USP9X and oxidative stress-induced cell death. Mol. Cell *36*, 805–818.

Nishitoh, H., Saitoh, M., Mochida, Y., Takeda, K., Nakano, H., Rothe, M., Miyazono, K., and Ichijo, H. (1998). ASK1 is essential for JNK/SAPK activation by TRAF2. Mol. Cell *2*, 389–395.

Noguchi, T., Takeda, K., Matsuzawa, A., Saegusa, K., Nakano, H., Gohda, J., Inoue, J., and Ichijo, H. (2005). Recruitment of tumor necrosis factor receptor-associated factor family proteins to apoptosis signal-regulating kinase 1 signalosome is essential for oxidative stress-induced cell death. J. Biol. Chem. *280*, 37033–37040.

Noguchi, T., Ishii, K., Fukutomi, H., Naguro, I., Matsuzawa, A., Takeda, K., and Ichijo, H. (2008). Requirement of reactive oxygen species-dependent activation of ASK1-p38 MAPK pathway for extracellular ATP-induced apoptosis in macrophage. J. Biol. Chem. *283*, 7657–7665.

Petroski, M.D., and Deshaies, R.J. (2005). Function and regulation of cullin-RING ubiquitin ligases. Nat. Rev. Mol. Cell Biol. *6*, 9–20.

Prag, S., and Adams, J.C. (2003). Molecular phylogeny of the kelch-repeat superfamily reveals an expansion of BTB/kelch proteins in animals. BMC Bioinformatics *4*, 42.

Saitoh, M., Nishitoh, H., Fujii, M., Takeda, K., Tobiume, K., Sawada, Y., Kawabata, M., Miyazono, K., and Ichijo, H. (1998). Mammalian thioredoxin is a direct inhibitor of apoptosis signal-regulating kinase (ASK) 1. EMBO J. *17*, 2596–2606.

Sekine, Y., Takagahara, S., Hatanaka, R., Watanabe, T., Oguchi, H., Noguchi, T., Naguro, I., Kobayashi, K., Tsunoda, M., Funatsu, T., et al. (2011). p38 MAPKs regulate the expression of genes in the dopamine synthesis pathway through phosphorylation of NR4A nuclear receptors. J. Cell Sci. *124*, 3006–3016.

Skinner, J., Sinclair, C., Romeo, C., Armstrong, D., Charbonneau, H., and Rossie, S. (1997). Purification of a fatty acid-stimulated protein-serine/threonine phosphatase from bovine brain and its identification as a homolog of protein phosphatase 5. J. Biol. Chem. *272*, 22464–22471.

Takeda, K., Noguchi, T., Naguro, I., and Ichijo, H. (2008). Apoptosis signal-regulating kinase 1 in stress and immune response. Annu. Rev. Pharmacol. Toxicol. *48*, 199–225.

Toba, G., Ohsako, T., Miyata, N., Ohtsuka, T., Seong, K.H., and Aigaki, T. (1999). The gene search system. A method for efficient detection and rapid molecular identification of genes in Drosophila melanogaster. Genetics *151*, 725–737.

Tobiume, K., Matsuzawa, A., Takahashi, T., Nishitoh, H., Morita, K., Takeda, K., Minowa, O., Miyazono, K., Noda, T., and Ichijo, H. (2001). ASK1 is required for sustained activations of JNK/p38 MAP kinases and apoptosis. EMBO Rep. *2*, 222–228.

Tobiume, K., Saitoh, M., and Ichijo, H. (2002). Activation of apoptosis signal-regulating kinase 1 by the stress-induced activating phosphorylation of pre-formed oligomer. J. Cell. Physiol. *191*, 95–104.

Widmann, C., Gibson, S., Jarpe, M.B., and Johnson, G.L. (1999). Mitogen-activated protein kinase: conservation of a three-kinase module from yeast to human. Physiol. Rev. *79*, 143–180.

Yamaguchi, Y., Katoh, H., Mori, K., and Negishi, M. (2002). Galpha(12) and Galpha(13) interact with Ser/Thr protein phosphatase type 5 and stimulate its phosphatase activity. Curr. Biol. *12*, 1353–1358.

Yang, J., Roe, S.M., Cliff, M.J., Williams, M.A., Ladbury, J.E., Cohen, P.T., and Barford, D. (2005). Molecular basis for TPR domain-mediated regulation of protein phosphatase 5. EMBO J. *24*, 1–10.

Zeke, T., Morrice, N., Vázquez-Martin, C., and Cohen, P.T. (2005). Human protein phosphatase 5 dissociates from heat-shock proteins and is proteolytically activated in response to arachidonic acid and the microtubule-depolymerizing drug nocodazole. Biochem. J. *385*, 45–56.

Biochemical and Biophysical Research Communications 428 (2012) 197–202

Contents lists available at SciVerse ScienceDirect

Biochemical and Biophysical Research Communications

journal homepage: www.elsevier.com/locate/ybbrc

Mitochondrial hexokinase HKI is a novel substrate of the Parkin ubiquitin ligase

Kei Okatsu [a,b], Shun-ichiro Iemura [c,d], Fumika Koyano [a,b], Etsu Go [a], Mayumi Kimura [a], Tohru Natsume [d], Keiji Tanaka [a,*], Noriyuki Matsuda [a,*]

[a] Laboratory of Protein Metabolism, Tokyo Metropolitan Institute of Medical Science, Setagaya-ku, Tokyo 156-8506, Japan
[b] Graduate School of Frontier Sciences, Department of Medical Genome Sciences, The University of Tokyo, Kashiwa, Chiba 277-8561, Japan
[c] Division of Translational Research for Drug Development, Fukushima Medical University, Hikariga-oka, Fukushima 960-1295, Japan
[d] Biomedicinal Information Research Center, National Institute of Advanced Industrial Science and Technology, 2-4-7 Aomi, Koto-ku, Tokyo 135-0064, Japan

ARTICLE INFO

Article history:
Received 28 September 2012
Available online 13 October 2012

Keywords:
Parkin
Ubiquitin
Mitochondria
Hexokinase
Parkinson disease

ABSTRACT

Dysfunction of Parkin, a RING-IBR-RING motif containing protein, causes autosomal recessive familial Parkinsonism. Biochemically, Parkin is a ubiquitin-ligating enzyme (E3) that catalyzes ubiquitin transfer from ubiquitin-activating and -conjugating enzymes (E1/E2) to a substrate. Recent studies have revealed that Parkin localizes in the cytoplasm and its E3 activity is repressed under steady-state conditions. In contrast, Parkin moves to mitochondria with low membrane potential, thereby activating the latent enzymatic activity of the protein, which in turn triggers Parkin-mediated ubiquitylation of numerous mitochondrial substrates. However, the mechanism of how Parkin-catalyzed ubiquitylation maintains mitochondrial integrity has yet to be determined. To begin to address this, we screened for novel Parkin substrate(s) and identified mitochondrial hexokinase I (HKI) as a candidate. Following a decrease in membrane potential, Parkin ubiquitylation of HKI leads to its proteasomal degradation. Moreover, most disease-relevant mutations of Parkin hinder this event and endogenous HKI is ubiquitylated upon dissipation of mitochondrial membrane potential in genuine-Parkin expressing cells, suggesting its physiological importance.

1. Introduction

Parkinson's disease (PD) is one of the most pervasive neurodegenerative diseases affecting 1% of the population over the age of 65. PD manifests as the dysfunction and loss of dopaminergic neurons in the *substantia nigra*, although neurons in other brain regions are also affected. PD commonly arises sporadically; however, in some cases the disease is familial and inherited. *PARKIN* is a causal gene for autosomal recessive early-onset parkinsonism [1] the product of which (the Parkin protein) functions as an enzyme responsible for substrate recognition and subsequent ubiquitin-ligation (i.e. E3 enzyme) [2].

Mitochondrial homeostasis plays a pivotal role in the maintenance of normal healthy cells, in particular non-dividing cells such as neurons. To maintain the integrity of mitochondria, the selective elimination of impaired mitochondria caused by various endogenous and exogenous stresses, such as unnecessary generation of reactive oxygen species (ROS) and mtDNA mutations, is critical [3,4]. Newly emergent evidence has shown that Parkin-dependent ubiquitylation plays a pivotal role in the quality control of mitochondria. The linkage between Parkin and mitochondria was first discovered in loss-of-function mutations in the fruit fly [5]. *Drosophila* that lack Parkin display severe defects in mitochondria [5]. Later, a reduction in the respiratory capacity of striatal mitochondria was demonstrated in parkin−/− mice [6]. In 2008, Richard Youle's lab reported that Parkin translocates to depolarized mitochondria and induces autophagic degradation of damaged mitochondria, a process termed mitophagy [7]. In 2010, several groups, including ours, reported that the recruitment of Parkin to impaired mitochondria requires PINK1, another early-onset hereditary PD gene product [8–11]. Following translocation to the mitochondrial surface, Parkin is converted to its active form [9] and ubiquitylates numerous substrates on the outer mitochondrial membrane (OMM) upon dissipation of the mitochondrial membrane potential ($\Delta\Psi_m$). Parkin has been shown to ubiquitylate a translocase component of the OMM complex (Tom70, Tom40 and Tom20), the pro-apoptotic factors BAK and BAX, mitochondrial Rho GTPases (MIRO) 1 and 2, mitochondrial fission factors FIS1 and Drp1, mitochondrial fusion factor Mitofusin (MFN), and voltage-dependent anion channel VDAC [8,12–22]. Additionally, high-throughput analysis revealed that many other proteins are downregulated upon Parkin expression in HeLa cells [23], implying that more substrates of Parkin exist. Collectively, Parkin seems to

* Corresponding authors. Address: Laboratory of Protein Metabolism, Tokyo Metropolitan Institute of Medical Science, 2-1-6 Kamikitazawa, Setagaya-ku, Tokyo 156-8506, Japan. Fax: +81 3 5316 3152.
E-mail addresses: tanaka-kj@igakuken.or.jp (K. Tanaka), matsuda-nr@igakuken.or.jp (N. Matsuda).

0006-291X/$ - see front matter © 2012 Elsevier Inc. All rights reserved.
http://dx.doi.org/10.1016/j.bbrc.2012.10.041

ubiquitylate diverse substrates, thus regulating multiple aspects of mitochondrial biology.

To further explore the molecular function of Parkin, we screened for cellular partner(s) that interact with Parkin following mitochondrial depolarization, and identified a novel substrate, hexokinase I (HKI), that had eluded previous identification in high-throughput analyses [23]. HKI is ubiquitylated by Parkin upon dissipation of mitochondrial membrane potential. Here, we present data suggesting that HKI is a novel Parkin substrate.

2. Materials and methods

2.1. Plasmids and reagents

Plasmids to express wild type Parkin and various pathogenic mutants have been described previously [9,24,25]. HKI and CISD1/mitoNEET were amplified by PCR from a brain cDNA library and were sub-cloned into pcDNA3.1-HA vector. Plasmid transfection was performed using FuGene6 (Roche). To depolarize the mitochondria, cells were treated with 10–15 μM CCCP (Sigma) for 1 h, unless otherwise specified. To inhibit proteolytic activity of the proteasome or the lysosome, 10 μM MG132 (Peptide Inc.) or 200 nM Bafilomycin A1 (Wako) was added simultaneously with CCCP for the indicated time. To inhibit protein translation, 50 μg/ml cycloheximide (Wako) was used. To allow for PINK1 accumulation, cells were treated with cycloheximide 30 min after CCCP treatment.

2.2. Protein identification by LC-MS/MS analysis

Flag-Parkin was expressed in HEK293 cells and immunoprecipitated using an anti-Flag antibody (M2). Parkin-associated proteins were digested with lysyl endopeptidase C (Lys-C, Wako) and the resulting peptides mixtures diluted 10-fold with 0.1% formic acid were analyzed by direct nanoflow liquid chromatography tandem mass spectrometry (DNLC-MS/MS) system [26] coupled to a QSTAR XL (AB Sciex). Peptides were separated on a C18 reversed-phase column packed with Mightysil C18 (particle size 3 μm; Kanto Chemical) by a 40-min linear gradient from 5% to 40% acetonitrile in 0.1% formic acid, and were sprayed on-line to the mass spectrometer. All MS/MS spectra were queried against the National Center for Biotechnology Information (NCBI) non-redundant database using an in-house Mascot server (Matrix Science).

2.3. Immunofluorescence (IF), immunoprecipitation (IP) and immunoblotting (IB)

To detect the ubiquitylation of VDAC1, HKI, CISD1/mitoNEET and Tom70 in immunoblots, cell lysates were collected in the presence of 10 mM *N-ethylmaleimide* to protect ubiquitylation from deubiquitylating enzymes. For IF experiments, cells were fixed with 4% paraformaldehyde, permeabilized with 50 μg/ml digitonin, and stained with primary antibodies described below and the following secondary antibodies: mouse and/or rabbit Alexa Fluor 488, 568, and 647 (Invitrogen). Cells were imaged using a laser-scanning microscope (LSM510; Carl Zeiss, Inc.). Image contrast and brightness were adjusted in Photoshop (Adobe). Antibodies used are as follows: anti-VDAC1 (Ab-3; Calbiochem), anti-actin (AC-40; Sigma), anti-hemagglutinin (HA) (6E2; Cell Signaling), anti-Parkin (PRK8; Sigma) and anti-ubiquitin (P4D1; Santa Cruz Biotech.) For IB, the following were used: anti-Flag (M2; Sigma), anti-HKI (C35C4; Cell Signaling), anti-HA (F7; Santa Cruz), and anti-Tom20 (FL-145 and F-10; Santa Cruz Biotech.). An anti-Tom70 antibody for IB [27] was provided by Drs. T. Otera, T. Oka, and K. Mihara (Kyushu University).

3. Results

3.1. Seven proteins were identified as Parkin-binding molecules following CCCP treatment

To identify novel Parkin substrate(s), we screened for proteins that interact with Parkinin response to a decrease in the mitochondrial membrane potential. N-terminal Flag-tagged Parkin was expressed in HEK293 cells, which were subsequently treated with the mitochondrial uncoupler carbonyl cyanide *m-chlorophenylhydrazone* (CCCP) and immunoprecipitated with an anti-Flag antibody. The immunoprecipitates were eluted with a Flag peptide and digested with Lys-C endopeptidase. The cleaved fragments were directly analyzed using a nano-flow LC-MS/MS system. Following a database search, a dozen peptides were assigned to MS/MS spectra obtained from four nano-LC-MS/MS analyses of the Flag-Parkin associated proteins. Finally, seven proteins were identified: three variants of a voltage-dependent anion channel 1 (VDAC1, VDAC2, and VDAC3), Tom70, a CDGSH iron sulfur domain-containing protein 1 (CISD1)/mitoNEET, non-metastatic cells 2 (NME2)/NM23B, and hexokinase I (HKI) (Table 1). Among those proteins, NME2/NM23B has been categorized in the UniProt database (http://www.uniprot.org/) as a cytoplasmic protein. The other six identified proteins have been categorized by both UniProt and MitoCarta databases [28] as predominantly mitochondrial. Given that Parkin localizes to mitochondria following CCCP treatment [7], we focused on these six mitochondrial proteins in the ensuing experiments.

3.2. VDAC1, CISD1 and HKI co-expressed with Parkin undergo modification following CCCP treatment

We next examined whether the aforementioned proteins undergo Parkin-mediated ubiquitylation following a decrease in the mitochondrial membrane potential. BecauseVDAC2 and VDAC3 show high sequence similarity (91% amino acid identity) to VDAC1, VDAC1 was used as the representative of these VDAC family proteins. HeLa cells lack a functional *PARKIN* gene [29] and thus exogenous HA-Parkin was introduced into HeLa cells. Interestingly, a higher molecular mass population of endogenous VDAC1 was observed following CCCP treatment in HA-Parkin expressing cells (Fig. 1A). The modification resulted in 6–7 kDa increase in the molecular weight of VDAC with the pattern strongly suggestive of ubiquitylation by Parkin, as has been reported previously [8]. There are currently no reliable antibodies capable of detecting endogenous CISD1/mitoNEET, we consequently fused a hemagglutinin (HA)-tag to the C-terminus of CISD1/mitoNEET to facilitate detection (note that the N-terminal portion of CISD1/mitoNEET is the domain for the mitochondrial outer-membrane anchor [30]) and was thus not selected for the epitope tag]. When CISD1/mitoNEET-HA and Parkin were co-expressed in HeLa cells, a higher molecular mass population of CISD1/mitoNEET-HA (putative ubiquitylated form) was also observed following CCCP treatment (Fig. 1B). In exogenous Parkin-expressing HeLa cells, a similar shift in the molecular weight of endogenous Tom70 was detected following CCCP treatment (Fig. 1C); however, that signal was much fainter than that of VDAC1 or CISD1/mitoNEET (compare Fig. 1C with 1A/1B). Finally, we examined HKI, an enzyme that phosphorylates six-carbon sugars and forms hexose-phosphates such as glucose-6-phosphate. Because the N-terminal region of HKI functions as the mitochondrial localization signal [31], a HA tag was fused to the C-terminus for subsequent detection and immunoprecipitation. When HKI-HA and Parkin wereco-expressed in HeLa cells, a higher molecular mass population of HKI was clearly observed following CCCP treatment. This modification was completely depen-

Table 1
Isolated proteins that potentially interact with Parkin.

Swiss-Prot accession number	Gene	Protein name	Subcellular localization	Previous report of physical and/or functional interaction
P2179	VDAC1	Voltage-dependent anion-selective channel protein 1	Mitochondria	Ref. [8,23]
P4588	VDAC2	Voltage-dependent anion-selective channel protein 2	Mitochondria	None
Q9Y277	VDAC3	Voltage-dependent anion-selective channel protein 3	Mitochondria	None
P19367	HKI	Hexokinase-1	Mitochondria	None
O94826	TOMM70A	Mitochondrial import receptor subunit Tom70	Mitochondria	Ref. [23]
Q9NZ45	CISD1	CDGSH iron-sulfur domain-containing protein 1 (MitoNEET)	Mitochondria	Ref. [23]
P22392	NME2/ NM23B	Nucleoside diphosphate kinase B	Cytoplasm	Ref. [23]

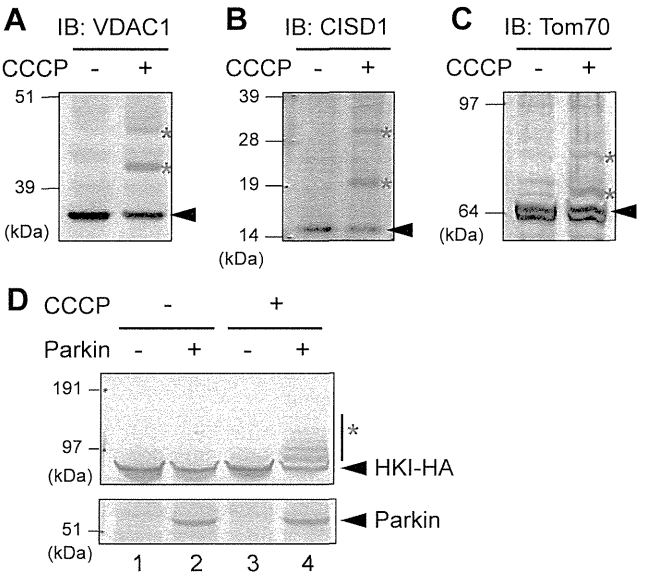

Fig. 1. (A–C) Isolated Parkin-interacting proteins underwent modification following a decrease in mitochondrial membrane potential. Endogenous VDAC1 (A), exogenous CISD1 (B) and endogenous Tom70 (C) were immunoblotted following CCCP treatment. (D) HeLa cells expressing both HKI and Parkin were treated with CCCP and then immunoblotted with the indicated antibodies. HKI underwent a ladder-like modification following Parkin and CCCP. Asterisks show Parkin-dependent modification.

dent on exogenous Parkin expression (Fig. 1D). In summary, VDAC1, CISD1/mitoNEET, and HKI were clearly modified, putatively via ubiquitylation, following a decrease in mitochondrial membrane potential whereas the signal for the modified Tom70 was much more faint. Ubiquitylation of VDAC1 and CISD1/mitoNEET following CCCP treatment have previously been reported [8,23], whereas ubiquitylation of HKI on depolarized mitochondria has not been reported. We thus selected HKI for further analyses.

3.3. Parkin-catalyzed ubiquitylation of hexokinase is blocked by pathogenic Parkin mutations

HKI-HA was immunoprecipitated with an anti-HA antibody and detected by anti-ubiquitin antibodies (Fig. 2A), demonstrating that the modification on HKI-HA was indeed ubiquitylation. We next examined the co-localization of Parkin and HKI in HeLa cells. Cells co-transfected with GFP-Parkin and HKI-HA were subjected to immunocytochemistry in the presence or absence of CCCP. An exogenous HKI-derived signal merged with a Tom20 signal irrespective of CCCP treatment, indicating the continuous mitochondrial localization of exogenous HKI, as reported previously [31]. GFP-Parkin localized throughout the cytoplasm under steady state conditions, but was transported to the mitochondria where it co-localized with HKI following CCCP treatment (Fig. 2B).

We next examined whether pathogenic mutations of Parkin affected the ubiquitylation of HKI. HA-Parkin mutants harboring one of eight pathogenic mutations (R42P, K161N, K211N, T240R, R275W, C352G, T415N and G430D) were serially introduced into HeLa cells with HKI-HA, followed by CCCP treatment for one hour, and the ubiquitylation of HKI analyzed. The R42P and R275W mutations destabilize exogenous Parkin, thus making interpretation of the results difficult because the diminution in HKI ubiquitylation is attributable to a decrease in mutant Parkin expression. Even though the expression of other pathogenic Parkin mutants was equivalent to wild type Parkin, HKI ubiquitylation in those cells was severely compromised (Fig. 2C). These results demonstrate that most of the pathogenic mutations of Parkin inhibit the ubiquitylation of HKI.

3.4. HKI is degraded by the proteasome following CCCP treatment

We next determined if HKI is destined for proteasomal degradation following Parkin-dependent ubiquitylation. HKI-expressing cells were treated with CCCP for 30 min (during this time PINK1 accumulates on mitochondria) and then subjected to CCCP and cycloheximide (CHX), an inhibitor of protein biosynthesis, simultaneously. In the presence of CHX, HKI underwent ubiquitylation one hour following CCCP treatment (Fig. 3A, lane 2) but gradually decreased over six hours (Fig. 3A, lanes 3,4). We thus examined whether the proteasomal inhibitor MG132 blocked the degradation of ubiquitylated HKI at six hours. When cells were treated with MG132, ubiquitylated HKI accumulated (Fig. 3B, compare lane 4 with 5) whereas treatment with bafilomycinA_1, an inhibitor of vacuolar-type H+-ATPase that prevents intra-lysosomal degradation, had no effect on the accumulation of ubiquitylated HKI (Fig. 3B, lane 6). These results suggest that Parkin-dependent ubiquitylation of HKI following dissipation of the mitochondrial membrane potential leads to its proteasomal degradation.

3.5. Endogenous HKI is ubiquitylated following CCCP treatment in cells expressing genuine Parkin

Although a clear ubiquitylation signal on HKI was observed (Fig. 2), the experimental conditions were artificial because both HKI and Parkin was over-produced to demonstrate the ubiquitylation. We thus used more stringent criteria to examine whether endogenous HKI is ubiquitylated following a decrease in the mito-

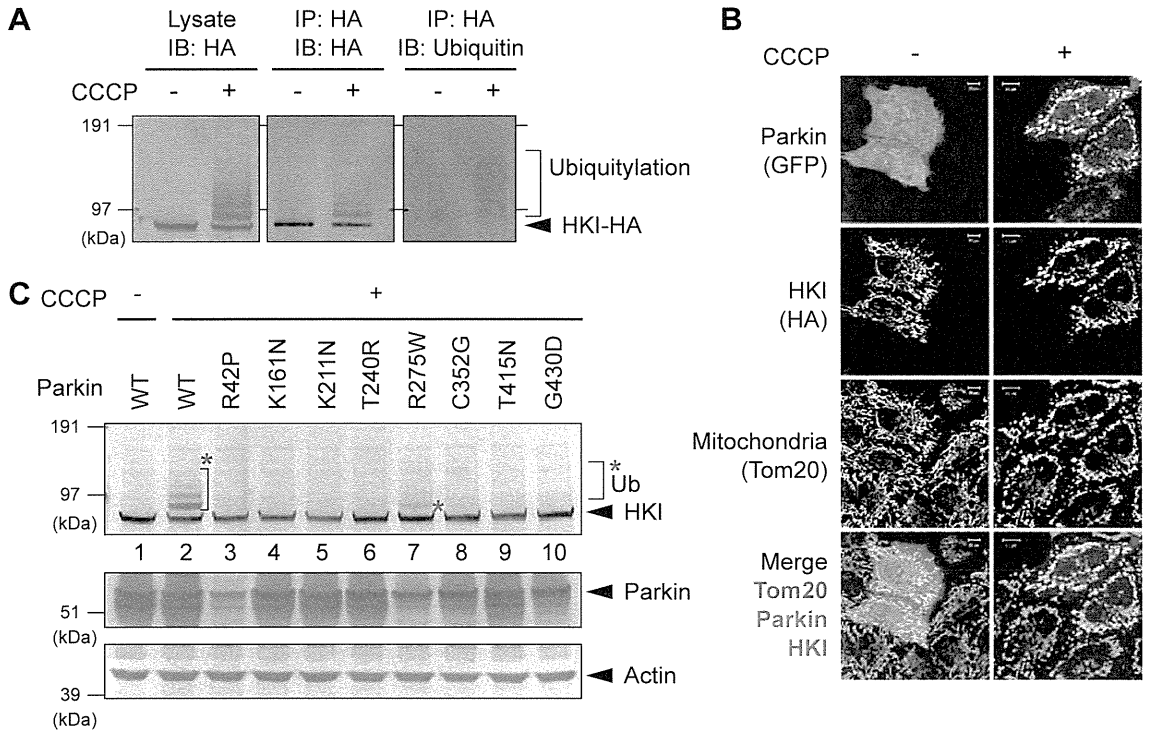

Fig. 2. HKI ubiquitylation on damaged mitochondria is inhibited by pathogenic mutations of Parkin. (A) HeLa cells expressing HKI-HA were treated with CCCP, immunoprecipitated with an anti-HA antibody and immunoblotted with anti-ubiquitin antibody. The result reveals that HKI is ubiquitylated. (B) HeLa cells expressing both GFP-Parkin and HKI-HA +/− CCCP treatment were immunostained. The results show that Parkin co-localized with HKI on damaged mitochondria. Bars, 10 μm. (C) HeLa cells expressing HKI and Parkin mutants were treated with CCCP and immunoblotted. HKI ubiquitylation was severely compromised by various pathogenic mutations in Parkin.

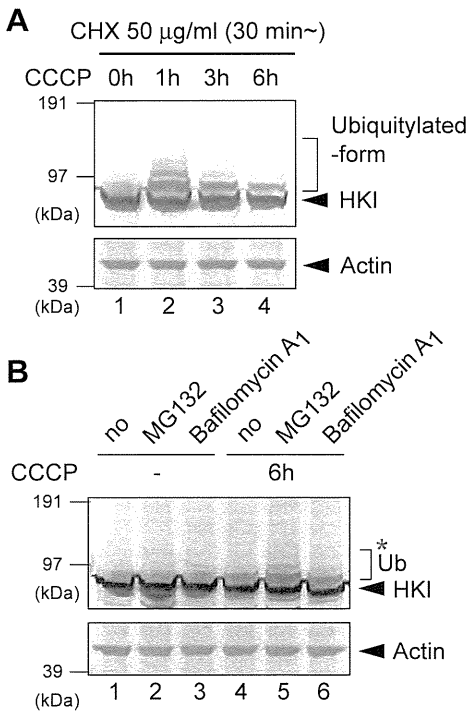

Fig. 3. (A) Degradation of HKI by the proteasome. HeLa cells were treated with CCCP and cycloheximide, and immunoblotted with the indicated antibodies. (B) Ubiquitylated HKI accumulated following treatment with MG132, a proteasome inhibitor. HeLa cells treated with CCCP, cyclohexmide and MG132 or Bafilomycin A1 were immunoblotted with the indicated antibodies.

chondrial membrane potential in cells expressing endogenous Parkin. As reported previously, HEK293 cells possess endogenous Parkin [32] and they also express endogenous HKI (Fig. 4A). When HEK293 cells were subjected to immunocytochemistry, endogenous HKI localized on mitochondria both in the presence and absence of CCCP (Fig. 4B), consistent with that of exogenous HKI (Fig. 2B). CCCP treatment of HEK293 cells resulted in a faint modification of HKI (Fig. 4C, a red asterisk). Clearer results were obtained following immunoprecipitation with an anti-HKI antibody. HKI was observed as doublet (Fig. 4C, a blue asterisk) and the upper band was detected with an anti-ubiquitin antibody (Fig. 4C, a black asterisk). We thus concluded that endogenous HKI also undergoes ubiquitylation in response to dissipation of the mitochondrial membrane potential in endogenous-Parkin-expressing cells.

4. Discussion

Our understanding of Parkin function has greatly expanded in recent years and shown to work with PINK1 to identify, label, clear and quarantine damaged mitochondria in cells (reviewed in [3,4,33]). Biochemically, Parkin functions as an E3 enzyme that catalyzes ubiquitin transfer from E1/E2~ubiquitin to the substrate [2,34–38]. Because PD is one of the most prevalent neurodegenerative disorders, the identification of Parkin substrates is important not only scientifically but also in terms of public welfare. Consequently, a number of Parkin substrates (>25) have been identified. However, there is one provision to most of these experiments, i.e. over-expressed Parkin and/or over-produced substrates were used to show the ubiquitylation. Studies without overexpression of the exogenous gene are extremely limited, excluding a few exceptions such as MFN [18].

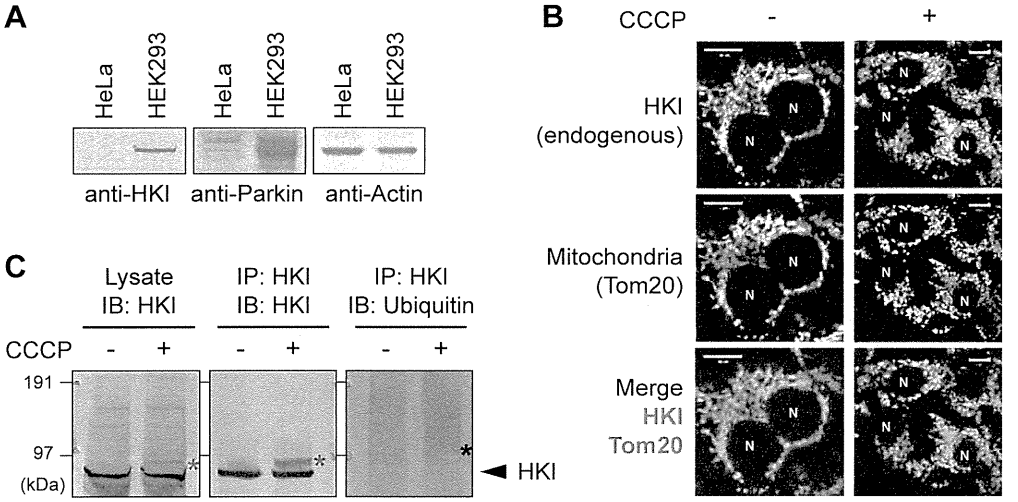

Fig. 4. (A) Expression of endogenous Parkin and HKI in HeLa and HEK293 cells. Actin was used as a loading control. (B) Immunocytochemistry of native HEK293 cells shows endogenous HKI localized on mitochondria regardless of CCCP treatment. N, nuclei; Bars, 10 μm. (C) Endogenous HKI was ubiquitylated following CCCP treatment in HEK293 cells. Lysates of untransfected HEK293 cells following CCCP treatment were immunoprecipitated with an anti-HKI antibody and immunoblotted with an anti-ubiquitin antibody.

To further reveal the function of Parkin, we sought to identify additional substrate(s) that are ubiquitylated following a decrease in mitochondrial membrane potential. In this study, we identified hexokinase I (HKI) as a candidate substrate. Exogenous HKI was ubiquitylated by exogenous Parkin (Fig. 1D). Moreover, we showed that endogenous HKI is also ubiquitylated upon dissipation of the mitochondrial membrane potential in Parkin-possessing cells (Fig. 4), whereas in cells lacking endogenous Parkin (e.g. HeLa cells) HKI is not ubiquitylated following CCCP treatment and exogenous-Parkin-expression is required for the ubiquitylation (Fig. 1). Attempts to use siRNA knockdown of endogenous Parkin in HEK cells were problematic as only a subtle decrease in the ubiquitylation of positive controls Mitofusin and Miro was observed (data not shown). We thus have not unequivocally demonstrated that endogenous HKI is ubiquitylated by endogenous Parkin following a decrease in the mitochondrial membrane potential in cells and further analysis will be required. Nevertheless, our results strongly suggest that HKI is a genuine novel substrate of Parkin.

Hexokinase plays a pivotal role in the cellular uptake and utilization of glucose. Hexokinase catalyzes the first obligatory step of glucose metabolism, namely the ATP-dependent phosphorylation of glucose to yield glucose-6-phosphate. Mammalian cells possess four highly homologous hexokinase isoforms, i.e. HKI, HKII, HKIII, and HKIV/glucokinase. HKI is predominantly expressed in the brain and the kidney, whereas HKII is expressed in muscle and adipose tissue. An important distinguishing feature of the HKI and HKII isoforms is mitochondrial localization via direct interaction with VDAC, the latter constituting a mitochondrial permeability transition pore (MPTP) [31,39]. We speculate that Parkin-catalyzed ubiquitylation of HKI perturbs MPTP function on depolarized mitochondria. In another scenario, hexokinase may link Parkin to the intracellular metabolic pathway, i.e. Parkin negatively regulates the pentose phosphate pathway and glycolysis via degradation of HKI. Interestingly, Van Laar et al. [40] reported that Parkin translocates to damaged mitochondria under glycolytic metabolism, whereas Parkin does not localize to depolarized mitochondria in cells forced into dependence on mitochondrial respiration. If so, then Parkin-mediated HKI degradation may inhibit glycolysis, and consequently Parkin's mitochondriallocalization is hindered, suggesting HKI functions as a negative feedback component.

Acknowledgments

We thank Drs. T. Otera, T. Oka, and K. Mihara (Kyushu University) for providing the anti-Tom70 antibody. This work was supported by Grant-in-Aid for JSPS Fellows (to K.O., Grant Number 23-6061), Grant-in-Aid for Young Scientists (A) (to N.M., JSPS KAKENHI Grant Number 23687018), Grant-in-Aid for Scientific Research on Innovative Area 'Brain Environment' (to N.M., MEXT KAKENHI Grant Number 24111557), the Takeda Science Foundation (to N.M. and K.T.), and Grant-in-Aid for Specially Promoted Research (to K.T., JSPS KAKENHI Grant Number 21000012).

References

[1] T. Kitada, S. Asakawa, N. Hattori, H. Matsumine, Y. Yamamura, S. Minoshima, M. Yokochi, Y. Mizuno, N. Shimizu, Mutations in the parkin gene cause autosomal recessive juvenile parkinsonism, Nature 392 (1998) 605–608.
[2] H. Shimura, N. Hattori, S. Kubo, Y. Mizuno, S. Asakawa, S. Minoshima, N. Shimizu, K. Iwai, T. Chiba, K. Tanaka, T. Suzuki, Familial Parkinson disease gene product, parkin, is a ubiquitin-protein ligase, Nat. Genet. 25 (2000) 302–305.
[3] O. Corti, S. Lesage, A. Brice, What genetics tells us about the causes and mechanisms of Parkinson's disease, Physiol. Rev. 91 (2011) 1161–1218.
[4] N. Exner, A.K. Lutz, C. Haass, K.F. Winklhofer, Mitochondrial dysfunction in Parkinson's disease: molecular mechanisms and pathophysiological consequences, EMBO J. 31 (2012) 3038–3062.
[5] J.C. Greene, A.J. Whitworth, I. Kuo, L.A. Andrews, M.B. Feany, L.J. Pallanck, Mitochondrial pathology and apoptotic muscle degeneration in Drosophila parkin mutants, Proc. Natl. Acad. Sci. USA 100 (2003) 4078–4083.
[6] J.J. Palacino, D. Sagi, M.S. Goldberg, S. Krauss, C. Motz, M. Wacker, J. Klose, J. Shen, Mitochondrial dysfunction and oxidative damage in parkin-deficient mice, J. Biol. Chem. 279 (2004) 18614–18622.
[7] D. Narendra, A. Tanaka, D.F. Suen, R.J. Youle, Parkin is recruited selectively to impaired mitochondria and promotes their autophagy, J. Cell Biol. 183 (2008) 795–803.
[8] S. Geisler, K.M. Holmstrom, D. Skujat, F.C. Fiesel, O.C. Rothfuss, P.J. Kahle, W. Springer, PINK1/Parkin-mediated mitophagy is dependent on VDAC1 and p62/SQSTM1, Nat. Cell Biol. 12 (2010) 119–131.
[9] N. Matsuda, S. Sato, K. Shiba, K. Okatsu, K. Saisho, C.A. Gautier, Y.S. Sou, S. Saiki, S. Kawajiri, F. Sato, M. Kimura, M. Komatsu, N. Hattori, K. Tanaka, PINK1 stabilized by mitochondrial depolarization recruits Parkin to damaged mitochondria and activates latent Parkin for mitophagy, J. Cell Biol. 189 (2010) 211–221.
[10] D.P. Narendra, S.M. Jin, A. Tanaka, D.F. Suen, C.A. Gautier, J. Shen, M.R. Cookson, R.J. Youle, PINK1 is selectively stabilized on impaired mitochondria to activate Parkin, PLoS Biol. 8 (2010) e1000298.
[11] C. Vives-Bauza, C. Zhou, Y. Huang, M. Cui, R.L. de Vries, J. Kim, J. May, M.A. Tocilescu, W. Liu, H.S. Ko, J. Magrane, D.J. Moore, V.L. Dawson, R. Grailhe, T.M. Dawson, C. Li, K. Tieu, S. Przedborski, PINK1-dependent recruitment of Parkin to mitochondria in mitophagy, Proc. Natl. Acad. Sci. USA 107 (2010) 378–383.

[12] M. Cui, X. Tang, W.V. Christian, Y. Yoon, K. Tieu, Perturbations in mitochondrial dynamics induced by human mutant PINK1 can be rescued by the mitochondrial division inhibitor mdivi-1, J. Biol. Chem. 285 (2010) 11740–11752.
[13] M.E. Gegg, J.M. Cooper, K.Y. Chau, M. Rojo, A.H. Schapira, J.W. Taanman, Mitofusin 1 and mitofusin 2 are ubiquitinated in a PINK1/parkin-dependent manner upon induction of mitophagy, Hum. Mol. Genet. 19 (2010) 4861–4870.
[14] L. Glauser, S. Sonnay, K. Stafa, D.J. Moore, Parkin promotes the ubiquitination and degradation of the mitochondrial fusion factor mitofusin 1, J. Neurochem. 118 (2011) 636–645.
[15] S. Liu, T. Sawada, S. Lee, W. Yu, G. Silverio, P. Alapatt, I. Millan, A. Shen, W. Saxton, T. Kanao, R. Takahashi, N. Hattori, Y. Imai, B. Lu, Parkinson's disease-associated kinase PINK1 regulates miro protein level and axonal transport of mitochondria, PLoS Genet. 8 (2012) e1002537.
[16] A.C. Poole, R.E. Thomas, S. Yu, E.S. Vincow, L. Pallanck, The mitochondrial fusion-promoting factor mitofusin is a substrate of the PINK1/parkin pathway, PLoS One 5 (2010) e10054.
[17] A. Rakovic, A. Grunewald, J. Kottwitz, N. Bruggemann, P.P. Pramstaller, K. Lohmann, C. Klein, Mutations in PINK1 and Parkin impair ubiquitination of Mitofusins in human fibroblasts, PLoS One 6 (2011) e16746.
[18] A. Tanaka, M.M. Cleland, S. Xu, D.P. Narendra, D.F. Suen, M. Karbowski, R.J. Youle, Proteasome and p97 mediate mitophagy and degradation of mitofusins induced by Parkin, J. Cell Biol. 191 (2010) 1367–1380.
[19] H. Wang, P. Song, L. Du, W. Tian, W. Yue, M. Liu, D. Li, B. Wang, Y. Zhu, C. Cao, J. Zhou, Q. Chen, Parkin ubiquitinates Drp1 for proteasome-dependent degradation: implication of dysregulated mitochondrial dynamics in Parkinson disease, J. Biol. Chem. 286 (2011) 11649–11658.
[20] X. Wang, D. Winter, G. Ashrafi, J. Schlehe, Y.L. Wong, D. Selkoe, S. Rice, J. Steen, M.J. LaVoie, T.L. Schwarz, PINK1 and Parkin target miro forphosphorylation and degradation to arrest mitochondrial motility, Cell 147 (2011) 893–906.
[21] S.R. Yoshii, C. Kishi, N. Ishihara, N. Mizushima, Parkin mediates proteasome-dependent protein degradation and rupture of the outer mitochondrial membrane, J. Biol. Chem. 286 (2011) 19630–19640.
[22] E. Ziviani, R.N. Tao, A.J. Whitworth, Drosophila parkin requires PINK1 for mitochondrial translocation and ubiquitinates mitofusin, Proc. Natl. Acad. Sci. USA 107 (2010) 5018–5023.
[23] N.C. Chan, A.M. Salazar, A.H. Pham, M.J. Sweredoski, N.J. Kolawa, R.L. Graham, S. Hess, D.C. Chan, Broad activation of the ubiquitin–proteasome system by Parkin is critical for mitophagy, Hum. Mol. Genet. 20 (2011) 1726–1737.
[24] K. Okatsu, T. Oka, M. Iguchi, K. Imamura, H. Kosako, N. Tani, M. Kimura, E. Go, F. Koyano, M. Funayama, K. Shiba-Fukushima, S. Sato, H. Shimizu, Y. Fukunaga, H. Taniguchi, M. Komatsu, N. Hattori, K. Mihara, K. Tanaka, N. Matsuda, PINK1 autophosphorylation upon membrane potential dissipation is essential for Parkin recruitment to damaged mitochondria, Nat. Commun. 3 (2012) 1016.
[25] K. Okatsu, K. Saisho, M. Shimanuki, K. Nakada, H. Shitara, Y.S. Sou, M. Kimura, S. Sato, N. Hattori, M. Komatsu, K. Tanaka, N. Matsuda, P62/SQSTM1 cooperates with Parkin for perinuclear clustering of depolarized mitochondria, Genes Cells 15 (2010) 887–900.
[26] T. Natsume, Y. Yamauchi, H. Nakayama, T. Shinkawa, M. Yanagida, N. Takahashi, T. Isobe, A direct nanoflow liquid chromatography-tandem mass spectrometry system for interaction proteomics, Anal. Chem. 74 (2002) 4725–4733.
[27] H. Otera, Y. Taira, C. Horie, Y. Suzuki, H. Suzuki, K. Setoguchi, H. Kato, T. Oka, K. Mihara, A novel insertion pathway of mitochondrial outer membrane proteins with multiple transmembrane segments, J. Cell Biol. 179 (2007) 1355–1363.
[28] D.J. Pagliarini, S.E. Calvo, B. Chang, S.A. Sheth, S.B. Vafai, S.E. Ong, G.A. Walford, C. Sugiana, A. Boneh, W.K. Chen, D.E. Hill, M. Vidal, J.G. Evans, D.R. Thorburn, S.A. Carr, V.K. Mootha, A mitochondrial protein compendium elucidates complex I disease biology, Cell 134 (2008) 112–123.
[29] S.R. Denison, F. Wang, N.A. Becker, B. Schule, N. Kock, L.A. Phillips, C. Klein, D.I. Smith, Alterations in the common fragile site gene Parkin in ovarian and other cancers, Oncogene 22 (2003) 8370–8378.
[30] S.E. Wiley, A.N. Murphy, S.A. Ross, P. van der Geer, J.E. Dixon, MitoNEET is an iron-containing outer mitochondrial membrane protein that regulates oxidative capacity, Proc. Natl. Acad. Sci. USA 104 (2007) 5318–5323.
[31] R.B. Robey, N. Hay, Mitochondrial hexokinases, novel mediators of the antiapoptotic effects of growth factors and Akt, Oncogene 25 (2006) 4683–4696.
[32] A.C. Pawlyk, B.I. Giasson, D.M. Sampathu, F.A. Perez, K.L. Lim, V.L. Dawson, T.M. Dawson, R.D. Palmiter, J.Q. Trojanowski, V.M. Lee, Novel monoclonal antibodies demonstrate biochemical variation of brain parkin with age, J. Biol. Chem. 278 (2003) 48120–48128.
[33] K.L. Lim, X.H. Ng, L.G. Grace, T.P. Yao, Mitochondrial dynamics and Parkinson's disease: focus on parkin, Antioxid. Redox Signaling 16 (2012) 935–949.
[34] K.C. Chew, N. Matsuda, K. Saisho, G.G. Lim, C. Chai, H.M. Tan, K. Tanaka, K.L. Lim, Parkin mediates apparent E2-independent monoubiquitination in vitro and contains an intrinsic activity that catalyzes polyubiquitination, PLoS One 6 (2011) e19720.
[35] Y. Imai, M. Soda, R. Takahashi, Parkin suppresses unfolded protein stress-induced cell death through its E3 ubiquitin-protein ligase activity, J. Biol. Chem. 275 (2000) 35661–35664.
[36] N. Matsuda, T. Kitami, T. Suzuki, Y. Mizuno, N. Hattori, K. Tanaka, Diverse effects of pathogenic mutations of Parkin that catalyze multiple monoubiquitylation in vitro, J. Biol. Chem. 281 (2006) 3204–3209.
[37] D.M. Wenzel, A. Lissounov, P.S. Brzovic, R.E. Klevit, UBCH7 reactivity profile reveals Parkin and HHARI to be RING/HECT hybrids, Nature 474 (2011) 105–108.
[38] Y. Zhang, J. Gao, K.K. Chung, H. Huang, V.L. Dawson, T.M. Dawson, Parkin functions as an E2-dependent ubiquitin-protein ligase and promotes the degradation of the synaptic vesicle-associated protein, CDCrel-1, Proc. Natl. Acad. Sci. USA 97 (2000) 13354–13359.
[39] J.G. Pastorino, J.B. Hoek, Regulation of hexokinase binding to VDAC, J. Bioenerg. Biomembr. 40 (2008) 171–182.
[40] V.S. Van Laar, B. Arnold, S.J. Cassady, C.T. Chu, E.A. Burton, S.B. Berman, Bioenergetics of neurons inhibit the translocation response of Parkin following rapid mitochondrial depolarization, Hum. Mol. Genet. 20 (2011) 927–940.

Molecular Cell
Article

RPA Assists HSF1 Access to Nucleosomal DNA by Recruiting Histone Chaperone FACT

Mitsuaki Fujimoto,[1] Eiichi Takaki,[1] Ryosuke Takii,[1] Ke Tan,[1] Ramachandran Prakasam,[1] Naoki Hayashida,[1] Shun-ichiro Iemura,[2] Tohru Natsume,[2] and Akira Nakai[1,*]
[1]Department of Biochemistry and Molecular Biology, Yamaguchi University School of Medicine, Minami-Kogushi 1-1-1, Ube 755-8505, Japan
[2]National Institutes of Advanced Industrial Science and Technology, Kohtoh-ku, Tokyo 135-0064, Japan
*Correspondence: anakai@yamaguchi-u.ac.jp
http://dx.doi.org/10.1016/j.molcel.2012.07.026

SUMMARY

Transcription factor access to regulatory elements is prevented by the nucleosome. Heat shock factor 1 (HSF1) is a winged helix transcription factor that plays roles in control and stressed conditions by gaining access to target elements, but mechanisms of HSF1 access are not well known in mammalian cells. Here, we show the physical interaction between the wing motif of human HSF1 and replication protein A (RPA), which is involved in DNA metabolism. Depletion of RPA1 abolishes HSF1 access to the promoter of *HSP70* in unstressed condition and delays its rapid activation in response to heat shock. The HSF1-RPA complex leads to preloading of RNA polymerase II and opens the chromatin structure by recruiting a histone chaperone, FACT. Furthermore, this interaction is required for melanoma cell proliferation. These results provide a mechanism of constitutive HSF1 access to nucleosomal DNA, which is important for both basal and inducible gene expression.

INTRODUCTION

The access of transcription factors to regulatory elements in vivo is strongly inhibited by the local chromatin structure, in which the nucleosome core is composed of 147 bp of DNA wrapped 1.65 turns around the histone octamer. A "pioneer" transcription factor is first able to access its target element in nucleosomal DNA when other factors cannot (Zaret and Carroll, 2011; Magnani et al., 2011). Transcription factors bind to the regulatory elements and recruit coactivator complexes, including chromatin-modifying enzymes and nucleosome-remodeling complexes that move or displace histones at the promoter (Weake and Workman, 2010). These complexes then facilitate recruitment of the general transcription factors and RNA polymerase II (Pol II) to form the preinitiation complex, followed by promoter clearance and release of paused Pol II into transcription elongation. Nucleosome-depleted regions are detected in yeast promoters, and regulatory regions in *Drosophila* and human chromosomes are also frequently nucleosome deficient (Yuan et al., 2005; Mavrich et al., 2008; Schones et al., 2008). Nucleosome-depleted regions are not only generated by unfavorable intrinsic histone-DNA interaction in vivo (Sekinger et al., 2005; Zhang et al., 2009), but also by multiple sequence-specific factors locally bound to the regions (Bai et al., 2011; Guertin et al., 2012). Nucleosome depletion allows transcription factors to access promoters during differentiation and in response to external stimuli; however, molecular mechanisms by which a first "pioneer" transcription factor accesses nucleosomal regulatory elements are not well known.

The heat shock response is characterized by the induced expression of genes coding for heat shock proteins (HSPs) and non-HSP proteins in response to heat shock (Richter et al., 2010; Hayashida et al., 2010) and is regulated by evolutionarily conserved heat shock factors (HSFs) that bind to heat shock response elements (HSEs) in eukaryotes (Wu, 1995). Transcriptional regulation of the response has been extensively studied as a model system of gene expression. Metazoan HSF1 remains as an inactive monomer in unstressed cells and is converted to an active trimer that binds to the HSE during heat shock (Morimoto, 2008; Akerfelt et al., 2010; Fujimoto and Nakai, 2010). However, HSF1 by itself cannot gain access to nucleosomal DNA (Becker et al., 1991; Taylor et al., 1991). In *Drosophila*, GAGA factor restricts nucleosome occupancy of the HSP70 promoter, allowing for the establishment of paused RNA polymerase II (Pol II) in non-heat shock condition and quick access of HSF upon heat shock (Fuda et al., 2009). HSF binding precipitates the rapid loss of nucleosomes within the body of *HSP70* (Petesch and Lis, 2008). It is also followed by the activation and spread of poly(ADP-ribose) polymerase, recruitment of elongation factors such as P-TEFb and Spt6, and histone-modifying enzymes such as Trithorax and CREB-binding protein (CBP) (Smith et al., 2004; Zobeck et al., 2010; Petesch and Lis, 2012). In contrast, in mammals, no mechanism of the opening of the chromatin structure has been revealed yet.

It was recently revealed that mammalian HSF1 stably binds to inflammatory genes, such as *IL-6*, before stimulation and opens the local chromatin structure to allow subsequent binding of activators or repressors (Inouye et al., 2007; Rokavec et al., 2012). HSF1 is a winged helix transcription factor (Littlefield and Nelson, 1999; Gajiwala and Burley, 2000), which is characteristic of some pioneer transcription factors such as FOXA1 and PU.1 (Magnani et al., 2011). These results suggested HSF1 as a candidate "pioneer" transcription factor at least for

Table 1. Identification and Functional Screening of HSF1-Binding Proteins

Category	Gene Name	Group[a]	Relative Induction of HSP70 by Gene Knockdown[b]
DNA replication/ repair	RPA1	Group A	0.27[c]
	RPA2	Group A	0.25[c]
	RPA3	Group A	None
	SSBP1	Group A	0.23[c]
RNA splicing	PRPF8	Group A	0.09[c]
	SNRNP200	Group A	0.14[c]
	EFTUD2	Group A	0.12[c]
	SNRPD3	Group A	None
	RBM28	Group A	None
Transcription factor	MAZ	Group A	None
	BANF1	Group A	None
	TFAM	Group A	None
	DACH1/DACH2	Group C	1.94[c]
	ATF1/CREM/ CREB1	Group D	0.4[c]
Signaling	IQGAP1	Group B	None
	RICTOR	Group C	0.26[c]
	CCDC88A	Group C	None
Cellular structure	STMN3	Group B	None
	SNX4	Group C	None
	NES	Group D	None
Protein modification	ZC3HAV1	Group B	0.51[c]
	SUMO2	Group D	None
Protein degradation	STUB1	Group C	None
	HECTD3	Group D	None
Transport	KPNA3	Group D	None
	KPNA4	Group D	None
Enzyme	CPVL	Group D	3.58[d]
	HADHA	Group D	None
Nucleotide metabolism	PRPS1/PRPS2/ PRPS3	Group B	None
Other	ZZEF	Group A	None

[a]Proteins were classified by conditions, in which the physical interaction was detected. A, all; B, control; C, heat shock; D, recovery.
[b]Heat shock induction. Gene knockdown was confirmed by RT-PCR to be 5%–20% of each control level. See also Figure S1.
[c]Heat shock: 42°C, 1 hr.
[d]Heat shock: 42°C, 1 hr; and 37°C, 6 hr.

some genes and prompted us to analyze the molecular mechanisms of HSF1 access to nucleosomal DNA. Here we report that HSF1 forms a complex with replication protein A (RPA), which is known to bind and stabilize single-strand DNA (ssDNA) regions during DNA replication and repair (Wold, 1997). We show that the HSF1-RPA complex stably binds to HSF1-target genes including *HSP70* in unstressed condition, by recruiting a histone chaperone, FACT (facilitates chromatin transcription), which displaces the histone H2A-H2B dimer (Avvakumov et al., 2011). Furthermore, this HSF1-RPA1 complex has a great impact on the roles of HSF1 in the regulation of protein homeostasis (proteostasis) capacity (Balch et al., 2008; Morimoto, 2008) and cancer cell proliferation (Dai et al., 2007).

RESULTS

Identification and Functional Screening of HSF1-Binding Proteins

To find factors that assist in HSF1 access to nucleosomal DNA, we identified thirty proteins that are coprecipitated with human HSF1-Flag in HEK293 cells by mass spectrometry and performed functional screening (Table 1, Figures S1A and S1B). Knockdown of nine genes (*RPA1*, *RPA2*, *SSBP1*, *PRPF8*, *SNRNP200*, *EFTUD2*, *ATF1/CREM/CREB*, *RICTOR*, and *ZC3HAV1*) that correspond to HSF1-binding partners decreased the HSP70 protein level during heat shock; in contrast, depletion of two genes (*DACH1/DACH2* and *CPVL*) increased HSP70 protein levels. Among these eleven genes (37%), we analyzed the roles of replication A (RPA) hetero-trimer complex (RPA1-RPA3), which is essential for DNA replication (Wold, 1997). Knockdown of *RPA1* or *RPA2* reduced mRNA levels of major HSPs, including HSP70, and HSE-driven reporter not only at an early step during heat shock, but also under control condition (Figures S1C–S1E). This effect was not due to blocking replication, because knockdown of another replication factor, proliferating cell nuclear antigen (PCNA) (Moldovan et al., 2007), did not affect the expression of HSP70 (Figure S1F). These results indicate that RPA complex is involved in HSF1-mediated basal expression of HSP70 and suggest that it might modulate the chromatin structure.

RPA1 Binds to a Wing Motif of the Winged Helix Transcription Factor HSF1

HSF1 stably formed a complex with a RPA heterotrimer before and after heat shock in HEK293 cells (Figures 1A and S2A). To find which component of the complex directly interacts with HSF1, we purified bacterially expressed HSF1 and RPA proteins. We found that HSF1 directly interacts with RPA1 but not with RPA2 or RPA3 (Figure 1B). Furthermore, RPA1 interacted with the DNA-binding domain of HSF1 (Figure 1C). Because amino acid sequences of the DNA-binding domain are highly conserved among HSF family members, we examined the interaction of RPA1 with other HSF family members and found that RPA1 interacts with HSF4, but not with HSF2 (Figure S2B). To further limit the interacting site, ten amino acids of the HSF1 DNA-binding domain, which are identical to those of HSF4 but not to those of HSF2, were substituted with either alanine or the corresponding amino acid of HSF2 (Figure 1D). Substitution of glycine at aa 87 in HSF1 with serine or alanine abolished the interaction with RPA1 without affecting its DNA-binding activity in vitro, whereas other substitutions, including that of glutamic acid at aa 85 and proline at aa 92, did not affect the interaction

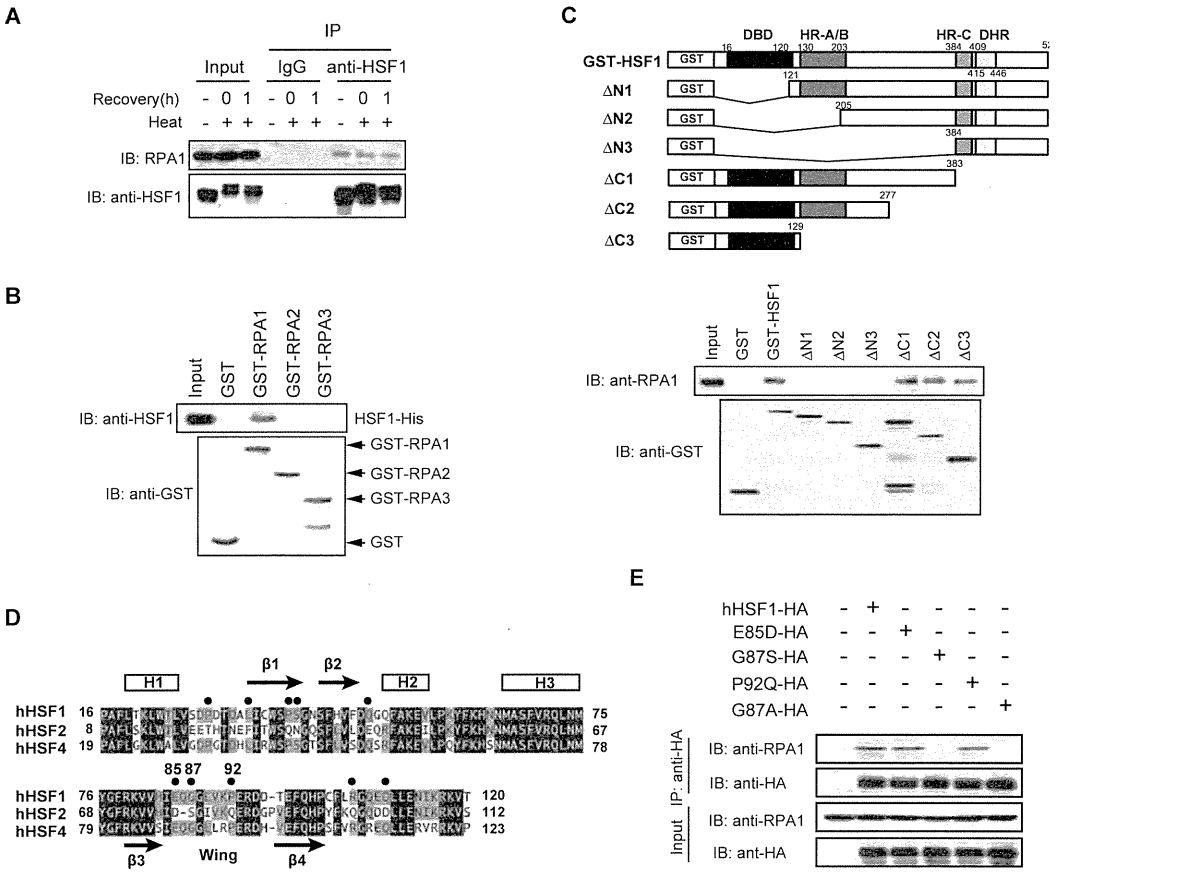

Figure 1. RPA1 Binds to the Wing Motif of HSF1 DNA-Binding Domain

(A) HSF1 interacts with endogenous RPA1 in HEK293 cells. Complexes coimmunoprecipitated with endogenous HSF1 in cells under control or heat shock condition were subjected to western blotting.

(B) HSF1 interacts directly with RPA1 in vitro. GST pull-down from mixtures of purified hHSF1-His and each GST-fused mRPA protein was performed, and proteins were subjected to western blotting.

(C) Schematic representation of hHSF1 deletion mutants fused to GST. The DNA-binding domain of HSF1 interacts with RPA1. GST pull-down from mixtures of purified mRPA1-His and GST fusion protein was performed, and proteins were subjected to western blotting. DBD, DNA-binding domain; HR, hydrophobic heptad repeat; DHR, downstream of HR-C.

(D) Alignment of the amino acid sequences of DNA-binding domains of hHSF1, hHSF2, and hHSF4. Predicted secondary structure is shown (Harrison et al., 1994; Vuister et al., 1994). Residues identical among three sequences are indicated in black, and those identical between only two are in gray. Ten residues in HSF1 that were similar to HSF4, but not HSF2, are indicated by dots, and some are indicated by numbers of amino acid residues.

(E) Interaction of RPA1 with HSF1 mutants. Each hHSF1 mutant tagged with HA was expressed in HEK293 cells, and complexes coimmunoprecipitated using HA antibody were subjected to western blotting (see also Figure S2).

(Figures 1E, S2C, and S2D). Furthermore, the EQG motif (aa 85–87) of HSF1 and the corresponding DS motif of HSF2 were swapped, and HSF2EGQ bound to RPA1, whereas HSF1DS did not (Figure S2E). These results indicate that the glycine at aa 87 in HSF1 is an interacting site to RPA1. This glycine is located in a disordered wing motif in the winged helix-turn-helix type DNA-binding domain of HSF1 (Littlefield and Nelson, 1999) and is evolutionally conserved among all of the eukaryotic HSF1 orthologs (Figure S2F).

RPA1 Is Required for HSF1 Access to HSP70 Promoter

There are proximal and distal HSEs (pHSE and dHSE, respectively) in human HSPA1A (HSP70-1) promoter, the sequences of which are evolutionally conserved in mammals (Figure 2A). HSF1 bound to both pHSE and dHSE with similar affinity in vitro (Kd = 2.50 and 2.77 nM, respectively) (Figure S3A). Addition of RPA proteins did not change the Kd values or cause the HSF1-HSE complexes to super shift at detectable levels (Figures S3A and S3B). Together these results suggest that RPA does not affect HSF1 binding to the HSE oligonucleotides in vitro. To examine the effects of RPA proteins on HSF1 binding to HSP70 promoter in vivo, we next performed a chromatin immunoprecipitation (ChIP) assay. We found that HSF1 binds only to pHSE in vivo in unstressed MEF cells (Figures 2B and 2C). HSF1 did not bind to the pHSE after knockdown of RPA1 or RPA2 (Figure 2C), whereas HSF1 binding was observed

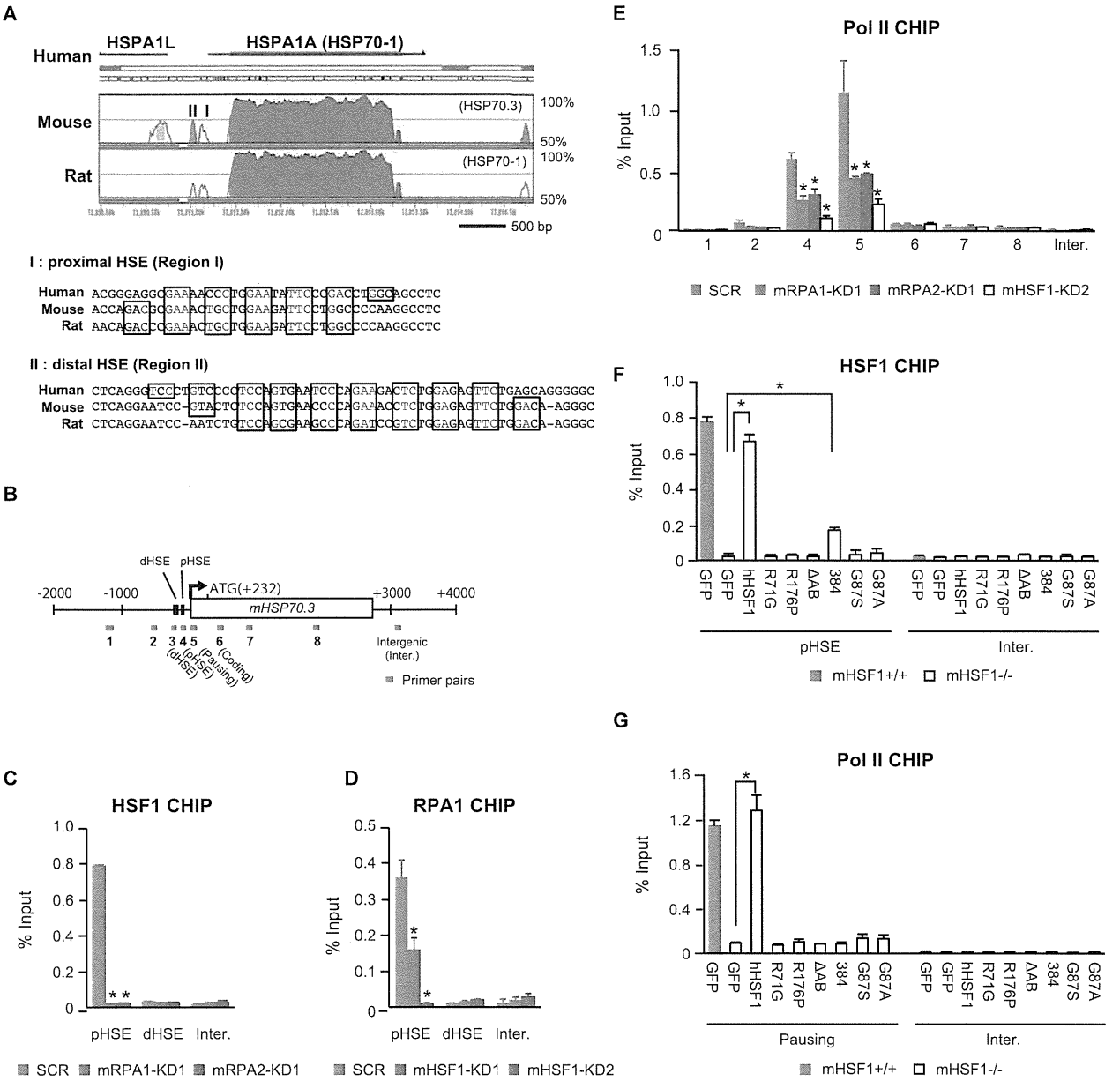

Figure 2. RPA Is Required for HSF1 Access to HSP70 Promoter and Pol II Preloading

(A) Alignment of sequences of human *HSPA1A* gene with those of mouse and rat orthologous genes. Genomic sequences were aligned with the VISTA program (http://genome.lbl.gov/vista/index.shtml), and percent identity is shown (upper). The proximal and distal HSEs are located in conserved promoter regions I and II, respectively (lower). Consensus nGAAn units are boxed, and conserved sequences are highlighted in red.

(B) Schematic representation of mouse HSP70.3 locus. Amplified DNA regions by real-time PCR are shown as numbered gray boxes.

(C) HSF1 constitutively binds to pHSE. MEF cells were infected with adenovirus expressing each shRNA, and ChIP analyses were performed using HSF1 antibody.

(D) RPA1 is recruited to the pHSE. MEF cells were infected with adenovirus expressing each shRNA, and ChIP-qPCR analyses were performed using RPA1 antibody.

(E) Pol II recruitment to the mouse HSP70.3 locus. MEF cells were infected with adenovirus expressing each shRNA, and ChIP-qPCR analyses were performed using Pol II antibody.

(F) Binding of hHSF1 mutants to HSP70 promoter. Wild-type hHSF1, each hHSF1 mutant, or GFP was expressed in wild-type (HSF1+/+) or HSF1 null (mHSF1−/−) MEF cells. ChIP-qPCR analyses of pHSE or an intergenic region were performed using HSF1 antibody.

(G) Recruitment of Pol II in the presence of hHSF1 mutants. MEF cells were treated as described in (F). ChIP-qPCR analyses of pausing and intergenic regions were performed using Pol II antibody. Error bars, SD (n = 3) in (C)–(G). Asterisks indicate $p < 0.01$ by Student's t test in (C)–(G) (see also Figure S3).